studies were conducted. Vesicular distributions of the ALS2 protein overlapped with those of endogenous EEA1, an early endosome marker (27) (Fig. 5B, ALS2_L/EEA1). Further, co-transfection of HeLa cells with expression constructs for the ALS2 protein and FLAG-tagged Rab5A demonstrated overlapped localization of the ALS2 protein with Rab5A onto the vesicular structures as well as cellular peripheries (Fig. 5B, ALS2_L/FLAG-Rab5A). These data indicate that a fraction of the ALS2 protein co-localizes with Rab5 onto the membranous compartments, particularly the early endosomes. Previous studies have shown that Rab5 acts cooperatively with EEA1 on early endosomes as a critical regulator in endosome fusions (28). Taken together, our findings imply a possible functional linkage between full-length ALS2 protein and Rab5 *in vivo*. Nonetheless, it is also evident that a majority of ALS2 molecules, at least in HeLa cells, exists in cytosol as possibly inactive or latent forms, because no obvious colocalization with Rab5 was observed (data not shown).

Overexpression of the ALS2 protein promotes endosome enlargement in cultured neuronal cells

To obtain further insights into the function of the ALS2 protein *in vivo*, rat primary cultured cortical neuronal cells were transfected with expression construct expressing the full-length ALS2 protein (Fig. 5C). It is noteworthy that the ectopically expressed ALS2 protein in Tau-positive neurons mostly spread throughout vesicles, which was in contrast to the diffused distributions in HeLa cells. We analyzed more than 100 neurons expressing the ALS2 protein, and ~90% of the cells revealed vesicular/patchy stainings in soma as well as in the elaborated somato-dendritic neurites (Fig. 5C, ALS2_L/Tau). Further, ALS2 localization onto some enlarged vacuolar vesicles were also seen (~10% of the cases; Fig. 5C, ALS2_L, arrowheads). A co-localization study with EEA1 demonstrated that the ALS2 protein localized onto EEA1-positive vesicular structures (Fig. 5C, middle panels; ALS2_L/EEA1), suggesting that the ALS2 protein functions on the early endosomal compartments in neurons (29). To obtain further evidence for the functional aspects of the ALS2 protein on early endosomes, co-transfection studies of cultured neuronal cells with expression constructs for the ALS2 protein and FLAG-tagged Rab5A were conducted. When the ALS2 protein and FLAG-Rab5A co-expressed, very enlarged endosomes, where the ALS2 protein coexisted with Rab5A, increased (Fig. 5C, ALS2_L/FLAG-Rab5A, arrowheads and enlarged images in the boxes), and those cells subsequently died prematurely. Taken together, overexpression of the full-length ALS2 protein in neuronal cells might promote endosome fusion/enlargement though the activation of the Rab5 within the endosomal compartments. Ectopic expression of a short variant of the ALS2 protein in cultured neurons revealed the diffused distributions in cytoplasm and nucleus (data not shown).

Molecular tropism and function for the ALS2 domains *in vivo*

To define the ALS2-domains responsible for the various subcellular localizations (diffused versus vesicular distributions), deletion constructs expressing the amino-terminally EGFP-fused ALS2 truncated mutants (Fig. 6A) were transfected into HeLa cells (Fig. 6B and C). EGFP-ALS2_1–680 amino acids carrying RLD showed a diffuse pattern of distribution with some patchy staining observed particularly in the perinulear area (Fig. 6B, EGFP_1–680), similar to the diffused-cases for full-length ALS2 (Fig. 6B, EGFP_ALS2L). Of particular note, a majority of the cases for EGFP-ALS2_660–1657 amino acids, containing the DH/PH/MORN/VPS9 region, revealed exclusive localization onto large-vacuolar structures (over ~2 μm in diameter; Fig. 6B, EGFP_660–1657) and/or EEA1-positive vesicles (Fig. 6B, EGFP_660–1657/EEA1), which was reminiscent of the enlarged endosomes observed in cultured neuronal cells and the Rab5_Q79L (a constitutive active form)-expressing cells (Fig. 6B, FLAG–Rab5A_CA). It has been reported that overexpression of Rab5_CA resulted in the enlarged vesicles with a typical size of 2–5 μm (30). These data suggest that ALS2_660–1657 amino acid fragment constitutively activates the endogenous Rab5 and promotes the drastic enlargement of early endosomes. EGFP-ALS2_1018–1657 amino acid (MORN/VPS9 domains), spanning a minimum region for the ALS2rab5GEF activity, also preferentially localized onto the EEA1-positive endosomes with the marginal enlargement (less than ~2 μm in diameter; Fig. 6B, EGFP_1018–1657/EEA1). The result was very similar to that obtained by the overexpression of the FLAG-tagged Rabex-5 (Fig. 6B, FLAG-Rabex-5). Further, EGFP-ALS2_1351–1657 amino acid fragments, lacking the Rab5-GEF activity, showed the similar degree of the vesicular localizations (Fig. 6B, EGFP_1351–1657). Consistent results were obtained for amino-terminally FLAG-tagged or the carboxy-terminally EGFP-fused ALS2 molecules in both COS-7 and HeLa cells (data not shown). These data suggest that each ALS2 domain/region demonstrates specific subcellular tropism *in vivo* (Fig. 6C). The amino-terminal RLD seems to confer cytosolic distribution, and thus could function as a negative regulator for the Rab5 binding and activation of Rab5. In contrast, the carboxy-terminus containing the VPS9 domain might mediate both Rab5 binding and endosomal localization. Notably the DH/PH constitutively promotes the MORN/VPS9-mediated Rab5

Figure 5. Ectopically expressed ALS2 showed overlapping distribution with Rab5 and EEA1 onto early endosome compartments in HeLa and rat cultured cortical neuronal cells. (A) Subcellular distribution of the ectopically expressed full-length (ALS2_L) or short form (ALS2_S) of the ALS2 proteins in HeLa cells. Three patterns of the ALS2 distributions are shown: patterns 1, 2, and 3. Arrowheads indicate the dense ALS2 stainings at the leading edges. The arrow indicates the ALS2 localization onto the enlarged vesicular structures. (B) Co-localization of ALS2_L with EEA1 or FLAG-tagged Rab5A. Left, middle and right columns represent ALS2_L, EEA1 or FLAG_Rab5A, and each merged image, respectively. Arrowheads indicate the dense ALS2 stainings at the leading edges or the cell peripheries. (C) Ectopically expressed full-length ALS2 in rat primary cortical neurons. The ALS2, EEA1, FLAG-tagged Rab5A and Tau proteins were immunofluorescently detected using anti-ALS2 polyclonal antibody (HPF1–680), anti-EEA1 monoclonal antibody FLAG-M2 monoclonal antibody and anti-Tau monoclonal antibody, respectively. Arrowheads indicate the ALS2 localization onto the enlarged vesicular structures. All the images were obtained by processing for immunofluorescence and analyzing by laser scanning confocal microscopy. Scale bars, 10 μm.

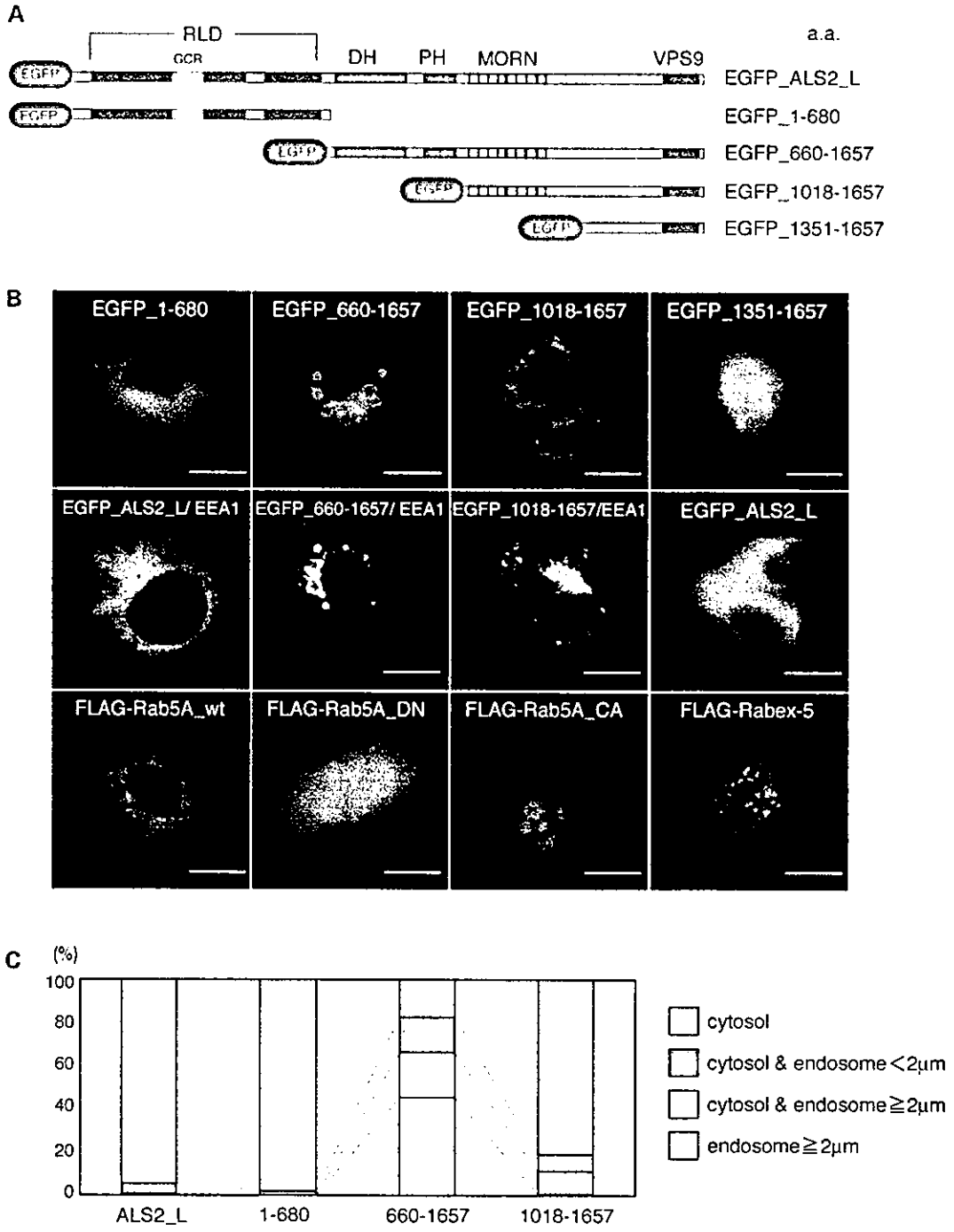

Figure 6. The ALS2 domains show distinct subcellular localizations and effects in HeLa cells. (A) A schematic diagram of the ALS2 protein and its truncated mutants used in the localization study. (B) Subcellular distribution of the ectopically expressed EGFP-fused proteins carrying distinct portions of ALS2 (EGFP–ALS2_1–680, EGFP–ALS2_660–1657, EGFP–ALS2_1018–1657, EGFP–ALS2_1351–1657 amino acids), full-length ALS2 (EGFP–ALS2_L), FLAG-tagged Rab5A [FLAG–Rab5A_wt (wild type), Rab5A_DN (dominant negative type; S34N), and Rab5A_CA (constitutive active type; Q79L)], and FLAG-tagged Rabex-5 in HeLa cells. Co-localization of the ALS2 fragments with endogenous EEA1were also shown (EGFP–ALS2_L/EEA1, EGFP_660–1657/EEA1 and EGFP_1018–1657/EEA1). All the images were obtained by processing for immunofluorescence and analyzing by laser scanning confocal microscopy. Scale bars, 20 μm. (C) Subcellular localization of the full-length and truncated ALS2 proteins and their effects on sizes of the ALS2-positive vesicular structures. Five hundred cells expressing each EGFP-fused ALS2 fragment were analyzed and counted. The percentages of the cell numbers revealing each localization phenotype are shown. The cells that showed the diffused ALS2 distributions were counted as 'cytosol'. The cells that showed vesicular ALS2 distributions were classified into two groups: 'endosome (<~2 μm)' represents the cells containing all the vesicles with less than ~2 μm in diameter (no and/or marginal enlargement); and 'endosome (≥~2 μm)' represents the cells revealing at least one of the vesicles with over ~2 μm in diameter (significant enlargement).

activation and endosome fusions *in vivo*, indicating the ALS2_660–1657 amino acid peptide might be a constitutive-active form for ALS2rab5GEF in the cells. Taken together, the Rab5-GEF activity associated with the full-length ALS2, ALS2rab5GEF, seems to be controlled by an internal domain(s) of ALS2 and implicated in the endosome dynamics *in vivo*.

Effect of the overexpression of the constitutive active form of the ALS2 protein on endosome dynamics

To delineate the molecular aspects of the ALS2rab5GEF activity on endosomal dynamics, we adopted overexpression of the ALS2_660–1657 amino acid peptide, a constitutive-active form for ALS2rab5GEF, in HeLa cells as a model system for the ALS2-activating status.

First, we examined the subcellular distribution of ectopically expressed ALS2_660–1657 amino acids. Co-localization was assessed with several other Rab family GTPases including Rab4A as early endosome markers (31,32), Rab7 as a late endosome marker (31,33,34) and Rab11A as a recycling endosome marker (31,35) (Fig. 7A). Co-transfection of HeLa cells with expression constructs for EGFP–ALS2_660–1657 amino acids and FLAG-tagged Rab4A, Rab7 and Rab11A demonstrated ALS2 protein co-localization with Rab4A (Fig. 7A, EGFP_660–1657/FLAG-Rab4A) and partially with Rab7 (Fig. 7A, EGFP_660–1657/FLAG-Rab7), but not with Rab11A (Fig. 7A, EGFP_660–1657/FLAG-Rab11A), indicating that ALS2_660–1657 amino acid peptide localizes predominantly onto the early endosome compartment and less frequently onto the late endosome, but not onto recycling endosome. ALS2_660–1657 amino acids did not localize to Golgi compartments by assessing the colocalization with GM130, a *cis*-Golgi marker (36) (data not shown).

To study whether the overexpression of ALS2_660–1657 amino acids affects endocytosis, HeLa cells transfected with ALS2_660–1657 amino acids expression construct were cultured in the presence of transferrin (Tfn) and epidermal growth factor (EGF), respectively, and distributions of these proteins within the cells were analyzed. ALS2_660–1657 amino acid and either Tfn or EGF predominantly co-localized onto the large vesicular compartments (Fig. 7B), consistent with the localization of the ALS2 peptides onto the actively internalized/endocytosed membrane compartments within the cells. On the other hand, ALS2_660–1657 amino acid peptide non-expressing cells observed in the same microscopic field only showed smaller Tfn- or EGF-positive vesicles without any evidence for endosome enlargement (Fig. 7B). These data also imply that overexpression of ALS2_660–1657 amino acids does not obstruct endocytosis of either Tfn or EGF, although it is still not clear whether trafficking of these molecules is disturbed within the cells.

To obtain insight into the effect of ALS2_660–1657 amino acids on the early/late endosomal dynamics, the distributions of two endosomal marker proteins, LAMP-1 and LAMP2, which were known as late endosome/lysosome markers (37,38), in cells expressing ALS2_660–1657 amino acids were analyzed. Overexpression of ALS2_660–1657 amino acids was associated with the accumulation of the lysosomal-associated membrane proteins LAMP-1 and LAMP-2 within the enlarged early endosome compartments (Fig. 7C). These data suggest an

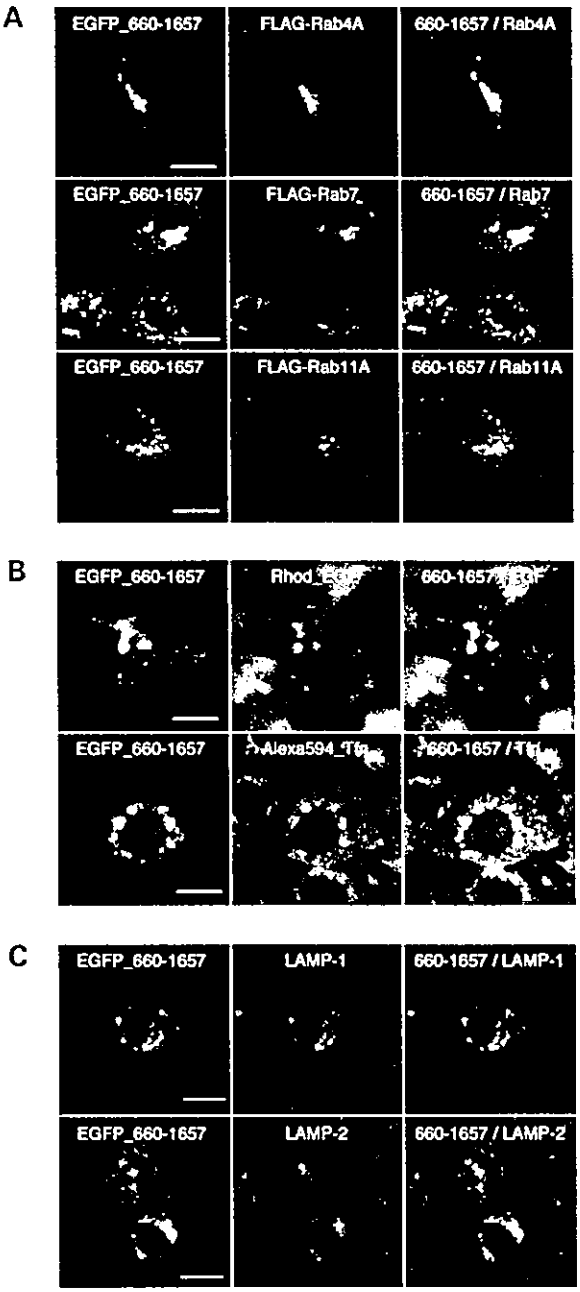

Figure 7. Effects of overexpression of ALS2_660–1657 amino acid peptide containing DH/PH domains on endosome dynamics in HeLa cells. (**A**) Confocal microscopic images of the HeLa cells ectopically co-expressed EGFP–ALS2_660–1657 amino acids (left-hand columns) and FLAG-tagged Rab family small GTPases (middle columns): FLAG-Rab4A, FLAG-Rab7 and FLAG-Rab11A. The right-hand columns display the merged images. (**B**) Colocalization of EGFP–ALS2_660–1657 amino acids (left-hand columns) and endocytic tracers; tetramedtylrhodamine-conjugated EGF (Rhod_EGF) (upper middle column) and Alexa 594-conjugated transferrin (Alexa594_Tfn) (lower middle column) onto enlarged endosomes in HeLa cells. Merged images are on the right. (**C**) Confocal microscopic immunofluorescence images for the ectopically expressed EGFP–ALS2_660–1657 amino acids (left-hand columns) and the endogenous organelle marker proteins (middle columns), including LAMP-1 (late endosome) and LAMP-2 (late endosome/lysosome) in HeLa cells. The right-hand columns display the merged images. Scale bars, 20 μm.

obstruction of lysosomal protein trafficking (39), possibly as a result of endosomal enlargement.

VPS9 domain functions as Rab5–GEF and contributes to the endosomal localization of the ALS2 protein

Given that protein sequence in the carboxy-terminal of the ALS2 protein functions as Rab5-GEF and localizes onto the enlarged endosome compartments, it was of particular interest to know whether the ALS2 protein is directly involved in endosome dynamics. We generated amino acid substituted mutants in which well-conserved amino acid residues among several VPS9 containing proteins were mutated (Fig. 8A): ALS2_660–1657 amino acid (P1603A) (proline at position 1603 to alanine) and ALS2_660–1657 amino acid (L1617A) (leucine at position 1617 to alanine). First, we assayed the GEF activity and GDP dissociation *in vitro* of these mutant proteins in the presence of Rab5A. Both mutations resulted in a marked decrease in GDP dissociation (Fig. 8B), implying that these amino acid residues are essential for ALS2rab5GEF activity. Next, we studied a subcellular localization of the ectopically expressed amino-terminally EGFP-fused mutant proteins in HeLa cells. EGFP–ALS2_660–1657 amino acids (P1603A) localized to as the same subcellular compartments as EGFP–ALS2_660–1657, _1018–1657 and _1351–1657 amino acids, without the enlargement of endosomes [Fig. 9A, EGFP_660–1657(P1603A)]. This suggests that ALS2_660–1657 amino acids (P1603A) fails in the endosome fusion by the loss of its GEF activity, although the mutant protein is recruited onto the endosomal compartments. By contrast, the EGFP–ALS2_660–1657 amino acids (L1617A) mutant scattered in cytosol [Fig. 9A, EGFP_660–1657(L1617A)], indicating that the L1617A mutation causes a loss of both ALS2rab5GEF activities and migration to the endosomal compartments.

ALS2 protein-induced enlargement of endosomal compartments is mediated by the activation of Rab5-EEA1 pathway

To examine whether ALS2_660–1657 amino acids directly activates small GTPase Rab5 and is involved in endosomal dynamics *in vivo*, co-expression experiments were undertaken with Rab5 proteins in HeLa cells. Transient expression of Rab5A_Q79L (constitutively active mutant) promoted the enlargement of endosomal compartments, while that of either Rab5A wild-type or Rab5A_S34N (dominant-negative mutant) provided the small and punctate vesicles (Fig. 6B, FLAG-Rab5A_wt or FLAG-Rab5A_DN), as reported previously (29,31,32). Co-expression of Rab5A_wt and ALS2_660–1657 amino acids revealed a prominent enlargement of endosomes (Fig. 9B, 660–1657/Rab5A_wt), indicating that the ectopically expressed Rab5A could be activated by ALS2rab5GEF to promote further enlargement of endosomes. This stimulatory effect was not seen when Rab5A_wt was co-expressed with ALS2_660–1657 amino acids (P1603A) [Fig. 9A, 660–1657(P1603A)/Rab5A_wt] or ALS2_660–1657 amino acids (L1617A) [Fig. 9A, 660–1657(L1617A)/Rab5A_wt]. Thus, the enlargement of endosomal compartments correlated closely with the activation of Rab5 GTPase by ALS2rab5GEF, suggesting a role for this protein in endosomal trafficking and

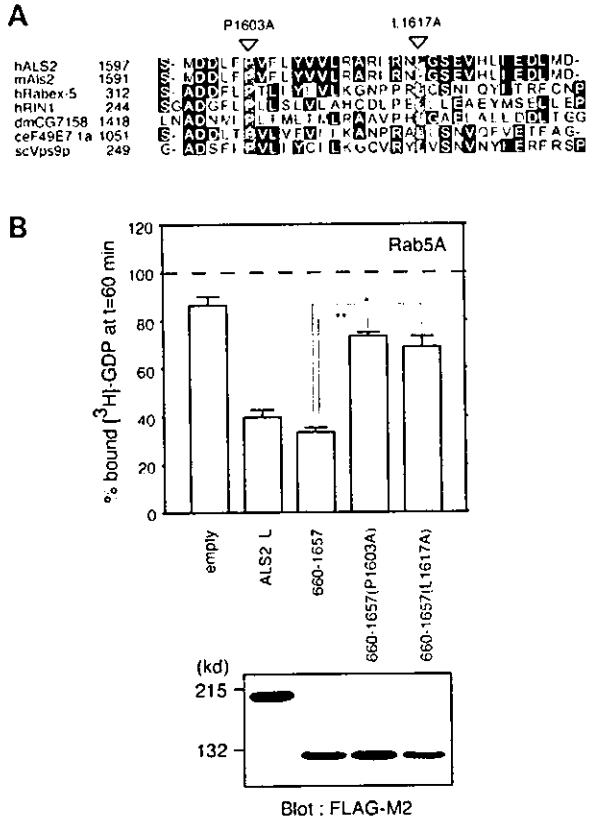

Figure 8. Effects of mutations in the VPS9 domain of the ALS2 protein on Rab5-GEF activity *in vitro*. (A) Multiple alignment of a portion of the VPS9 domains in the deduced ALS2 protein sequence. For VPS9 domains, human ALS2 (hALS2_VPS9), mouse ALS2 (mALS2_VPS9), human Rabex-5 (hRabex-5, ref; NP_055319), human Ras inhibitor RIN1 (hRasinhibitor, ref; NP_004283), *D. melanogaster* CG7158 (dmCG7158, gb; AAF51764), *C. elegans* F49E7.1a (ceF49E7.1a) and *S. cerevisiae* Vps9p (scVps9p, ref; NP_013612) are aligned. The black and gray shading represents identical and conserved amino acids, respectively. Sequences are numbered with the initiation codon of each protein as no. 1. The red shading represents the amino acids mutated in this study. (B) The [^{3}H]GDP dissociation assay *in vitro* using mutant ALS2 proteins: ALS2_660–1657, ALS2_660–1657(P1603A) and ALS2_660–1657 amino acids (L1617A). Western blotting of the immunoprecipitated FLAG-tagged ALS2 and its mutants used in this study are also shown. The percentage of [^{3}H]GDP that remained bound to Rab5A after 60 min is presented. Each value represents the mean and standard deviation of at least three independent assays. $^{**}P < 0.0001$; $^{*}P < 0.001$ in *t*-tests.

fusion via activation of members of small GTPase Rab5 family. Unexpectedly, overexpression of the dominant-negative Rab5A mutant, Rab5A_S34N, did not eliminate the enlarged endosomes in this experimental model (data not shown). It may be that the overexpressed ALS2 peptide activates enough endogenous Rab5 GTPases or alternative downstream pathway(s) to permit endosomal enlargement.

To further strengthen our findings of ALS2rab5GEF activity, a dominant-negative form of the carboxy-terminus of EEA1 (EEA1_1270–1411 amino acids) (40), a well-characterized Rab5 downstream effector (28,41) was used. When EGFP–ALS2_660–1657 amino acids was co-expressed with FLAG–EEA1_1270–1411 amino acids, enlargement of

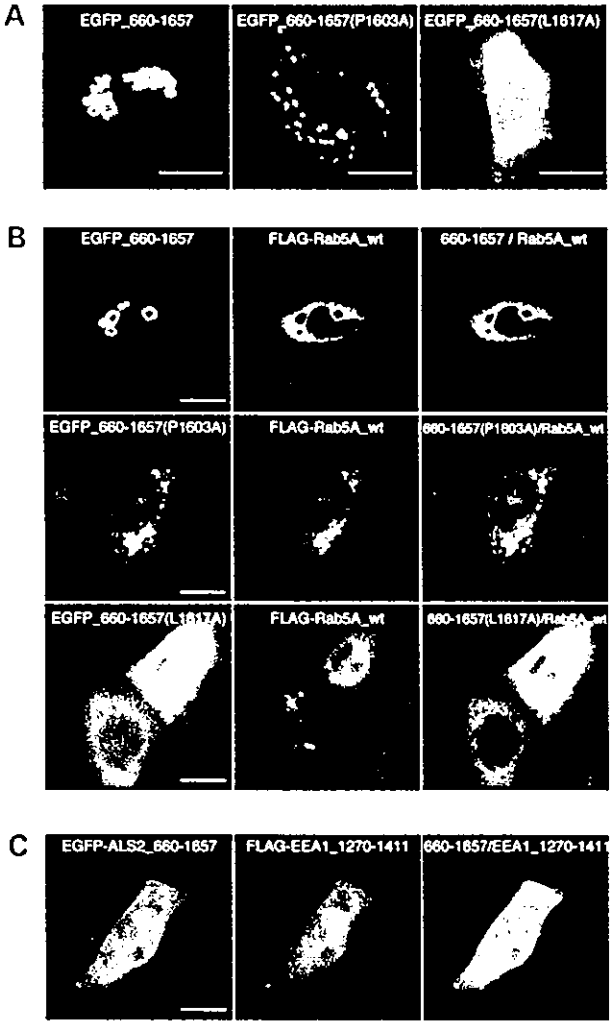

Figure 9. ALS2-promoted enlargement of endosomes is mediated by the activation of the Rab5–EEA1 pathway. (A) Effects of mutations in the VPS9 domain of the ALS2 protein on its intracellular distribution and endosome dynamics. Subcellular distribution of the ectopically expressed EGFP–ALS2_660–1657 (left), EGFP–ALS2_660–1657(P1603A) (middle) and EGFP–ALS2_660–1657 amino acids (L1617A) (right) in HeLa cells. (B) Co-expression of EGFP–ALS2_660–1657 (upper left), EGFP–ALS2_660–1657(P1603A) (middle left) or EGFP–ALS2_660–1657 amino acids (L1617A) (lower left) with FLAG–Rab5A_wt (middle) in HeLa cells. Merged images are shown in the right-hand columns. (C) Expression of the FLAG-tagged dominant-negative form of carboxy-terminal EEA1 fragment (FLAG–EEA1_1270–1411 amino acids) abrogates the ALS2-induced endosome enlargements. The left, middle and right columns display the images for EGFP–ALS2_660–1657, FLAG-EEA1_1270–1411 individually, and merged, respectively. Scale bars, 20 μm.

endosomes was completely suppressed (Fig. 9C). This indicates that ALS2rab5GEF involves inactivation of the Rab5–EEA1 pathway upstream of EEA1.

DISCUSSION

To our knowledge, the ALS2 protein is the fourth mammalian Rab5-specific GEF to be identified. The presence of a VPS9 domain in all four Rab5-GEFs (12–16) suggests that the essential GDP/GTP exchanging reaction may be conferred by this domain. A series of our deletion and mutagenesis studies revealed that the VPS9 domain of the ALS2 protein is a requisite for not only GDP/GTP exchange in Rab5 GTPase, but also endosomal targeting of the ALS2 protein. We have also demonstrated that the MORN motifs, although not essential for Rab5 binding, are necessary to fully activate ALS2rab5GEF. These data strongly suggests that VPS9 domain is working in conjunction with MORN co-operatively in the activation of the Rab5GTPases.

We have also documented the presence of regulatory elements and several GEF domains within the ALS2 molecule. The RLD appears to suppress recruitment of the full-length ALS2 protein onto endosomes and/or other membrane compartments in the cells. In contrast, the DH/PH domains appear to enhance MORN–VPS9 domain-mediated endosome fusion. A semi-quantitative analysis of the GDP dissociation *in vitro* revealed that the ALS2_660–1657 amino acid peptide containing DH/PH domains resulted in evident Rab5GEF activity which is significantly higher than that obtained with ALS2_1018–1657 amino acid peptide spanning a minimum region conferring the ALS2rab5GEF activity (Fig. 3C). This suggests that DH/PH could enhance ALS2rab5GEF activity resulting in a prominent endosome fusion. However, Rabex-5, a well-characterized Rab5-GEF (13,42), did not show significant endosome enlargement effects, despite its higher Rab5-GEF activity *in vitro* (Fig. 3C) and endosomal localization (Fig. 6B). We cannot rule out the possibility that the absence of endosome enlargement was due to insufficient levels of factors such as Rabaptin-5 known to interact with Rabex-5 (13,42). Nevertheless, it is clear that ALS2 and Rabex-5 proteins have differential effects on endosome dynamics in the cultured cells, suggesting that the multiple functional domains of the ALS2 protein in conjunction with unique upstream and/or downstream factors result in the leading of the intrinsic ALS2 function(s) and distribution.

Based on these results and endosomal dynamics (24,43–45), we propose the following physiological ALS2 function model (Fig. 10). Normally, RLD (RCC1-like domain) holds ALS2 proteins dispersed in the cytoplasm by means of an inter- and/or intra-RLD molecule association with the MORN-VPS9 region. In this situation, the majority of the cytosolic Rab5 molecules are maintained in GDP-bound inactive forms associated with Rab–GDI (GDP dissociation inhibitor) (46). An as yet unidentified molecular signal(s) inactivates RLD and activates MORN-VPS9 domain, initiating the recruitment of the ALS2 protein to the early endosomal compartments, where the ALS2 protein binds to a member of Rab5 small GTPases. The ALS2rab5GEF in the MORN-VPS9 domains of ALS2 then activates Rab5–GTPase through GDP/GTP exchange. The activated Rab5 further facilitates the formation of protein complex comprising downstream effector molecules such as EEA1 and SNARE (soluble *N*-ethylmaleimide-sensitive factor attachment protein receptor) proteins, promoting the endosomal fusion (47). Further, the ALS2 protein, particularly the DH/PH domain, could directly or indirectly up-regulate endosomal fusion.

Thus far, eight different mutations resulting in three distinct but phenotypically overlapping MNDs (ALS2, PLSJ and HSP)

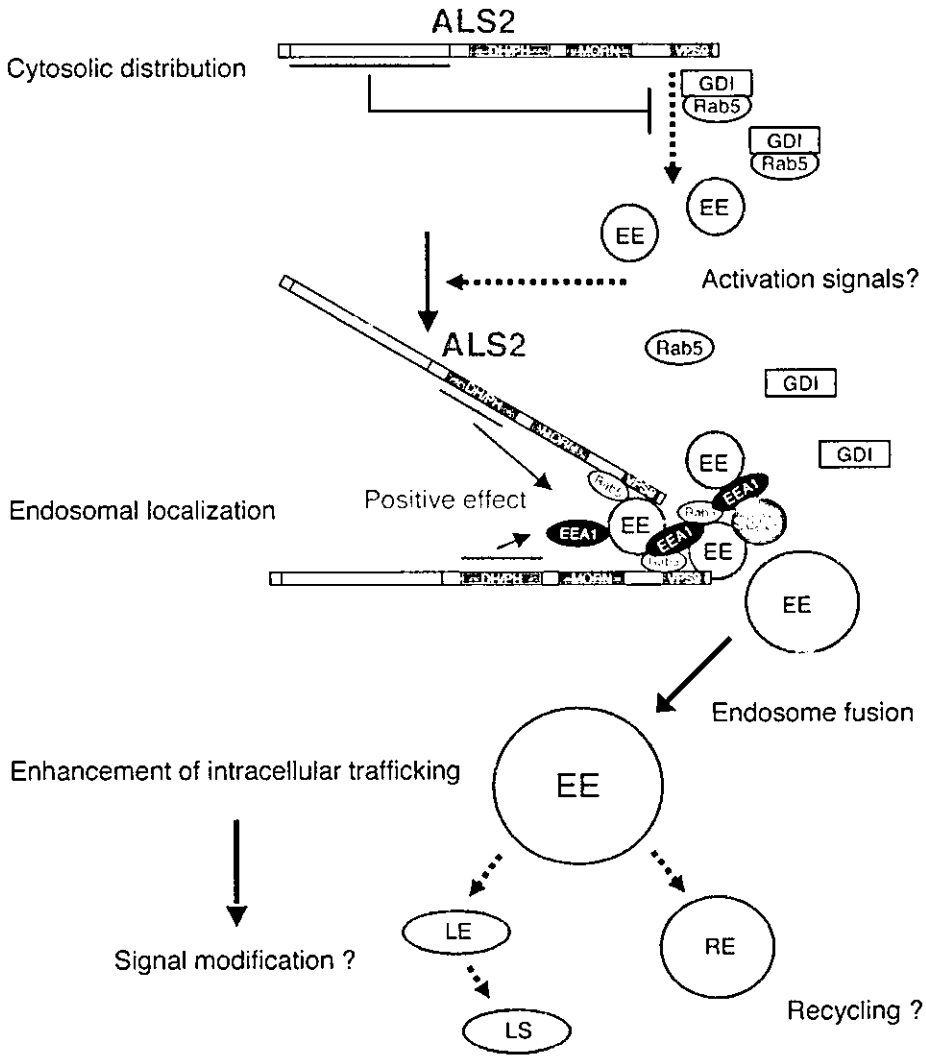

Figure 10. Proposed models for the ALS2 function and its implication in endosome dynamics. Pending a certain signal activation of the ALS2 molecule, RLD holds the ALS2 molecule dispersed in the cytoplasm by means of an inter- and/or intra-RLD molecule association with the MORN–VPS9 region. The majority of the Rab5 molecules exist in a GDP-bound inactive form associated with Rab–GDI. A particular molecular signal(s) (unidentified as yet) inactivates RLD and subsequently triggers MORN–VPS9 domains to recruit the ALS2 molecule for early endosomal compartments, wherein the ALS2 molecule binds to a member of Rab5 small GTPases. The ALS2rab5GEF in the MORN–VPS9 domains of the ALS2 protein activates Rab5–GTPase through GDP/GTP exchange. Activated Rab5 further facilitates the formation of protein complex comprising downstream effector molecules such as EEA1 and SNARE proteins, and promotes endosomal fusion. Further, the DH/PH domain could directly or indirectly up-regulate the fusion reactions. The ALS2 protein may also enhance certain intracellular transport of particular proteins and/or lipids and endosome-mediated signal transductions. In MND, loss of ALS2rab5GEF activity might disrupt endosomal trafficking and fusion, thereby resulting in the dysfunction and degeneration of the neuronal cells. GDI, Rab-GDP dissociation inhibitor; EEA1, early endosome antigen 1; SNARE, soluble *N*-ethylmaleimide-sensitive factor attachment protein receptor; EE, early endosome; LE, late endosome; RE, recycling endosome; LS, lysozome.

have been found in the *ALS2* gene (1,2,5,6). All the reported mutations cause disruption of the reading frame. A feature common to all ALS2–MND mutations is the loss of VPS9 domain, implicating ALS2rab5GEF function in endosome dynamics as being critical for motoneuron survival. This interpretation is consistent with the 4844delT mutation (4721delT; according to the den Dunnen's recommendations, www.DMD.nl/mutnomem.html) found in Pakistani kindred with HSP, which is predicted to result in a VPS9-functionless ALS2 protein, lacking half of the VPS9 domain at the carboxy-terminus (7). This *ALS2* gene mutation shows that loss of VPS9 domain (and loss of ALS2rab5GEF activity) is sufficient to

cause motor neuron death. The molecular mechanisms underlying phenotypic differences among ALS2, PLSJ and HSP, particularly LMN involvement, are still unclear at this stage. However, the uniform distribution of the short ALS2 protein variant both in cytoplasm and nucleus, which was completely different from those for the full-length ALS2 protein, could contribute to the phenotypic modulation.

Our functional model of the ALS2 protein may explain the unique molecular properties of the protein *in vivo*, and the selective or preferential dysfunction/degeneration of UMN resulting from the loss of rather widely expressed ALS2 proteins in patients with *ALS2* mutations. Notably, overexpression of the full-length ALS2 protein induced drastic enlargement of endosomes only in cultured neuronal cells, but not in HeLa or COS-7 cells. This suggests that a certain type of neuronal cell could be more amenable to the activation of the ALS2-mediated signaling pathways, and thus the devastating effects due to a loss of normal ALS2 protein could become more prominent in such neurons. Such a neuropathic effect of reduced or altered ALS2 function may involve the transport of neuronally specific macromolecules (e.g. proteins and/or lipids) or alter endosomally mediated signal transduction (48,49).

The recent identification of a number of causative genes has demonstrated that defective intracellular trafficking might underlie different forms of MNDs. In particular, the mutated genes for four types of HSPs, including SPG3A (50), SPG4 (51), SPG10 (52) and SPG20 (53), are all thought to directly involve intracellular trafficking (50–55). In addition, mutations in *KIF1Bβ*, which encodes a kinesin motor protein, and Rab7 result in Charcot–Marie–Tooth type 2A (OMIM 118210) (56) and type 2B (OMIM 600882) (57), respectively. Both are common inherited peripheral neuropathies. Defects in axonal transport and cytoskeletal organization have also been seen in sporadic as well as some familial ALS (58,59). Combining these result with our findings that the ALS2 protein functions as Rab5–GEF (ALS2rab5GEF), malfunction of the ALS2rab5GEF could obstruct membrane organization and endosomal dynamics, including endosome trafficking and fusion, and is implicated in ALS2, PLSJ and HSP.

MATERIALS AND METHODS

Antibodies

Anti-ALS2 rabbit antisera were raised by immunizing Japanese White rabbits with peptide (HPP1024; human ALS2 1024–1040 amino acids: QRQEPPISRSAKYTFYK) coupled to keyhole limpet hemocyanin via an amino-terminal cysteine residue, or with the purified His-tagged human ALS2_RLD fragment (HPF1-680; 1–680 amino acids). Each polyclonal antibody was affinity-purified using an antigen-coupled sepharose column. Other antibodies used in this study included anti-Flag monoclonal antibody M2 (1:3000; Stratagene), anti-GST monoclonal antibody (1:3000; Santa Cruz), anti-Rab4 monoclonal antibody (1:1000; Transduction Laboratories), anti-Rab5 monoclonal antibody (1:1000; Transduction Laboratories), anti-Rab11 monoclonal antibody (1:500; Transduction Laboratories), anti-EEA1 monoclonal antibody (1:100; BD biosciences), anti-GM130 monoclonal antibody (1:500; BD biosciences), anti-LAMP-1 monoclonal antibody (1:100; BD biosciences), anti-LAMP-2 monoclonal antibody (1:250; BD biosciences), anti-Tau monoclonal antibody (1:100; CalBioChem) and anti-β-tubulin monoclonal antibody (1:20 000; CHEMICON).

Western blot analysis

Whole-tissue extracts were prepared from fresh mouse tissues by homogenizing in lysis buffer [25 mM Tris–HCl; pH 7.5, 5 mM $MgCl_2$, 50 mM NaCl, 1 mM dithiothreitol (DTT), 5% (w/v) sucrose, 1% (w/v) IGIPAL CA-630, protease inhibitor cocktail (Roche), 1 mM phenylmethylsulfonyl fluoride (PMSF)], denatured in SDS sample buffer, subjected to SDS–PAGE, and transferred onto a PVDF membrane. Protein samples for the human cerebral cortex and cerebellum were purchased from BIOCHAIN Inc. Blots were incubated with anti-ALS2 antibodies (1:2000) or anti-β-tubulin antibody for 2 h, and with horseradish peroxidase-conjugated anti-rabbit or anti-mouse IgG sheep secondary antibody (Amersham Pharmacia), and developed using the ECL-plus kit (Amersham Pharmacia).

Plasmid constructs

All cDNA clones used in this study were obtained by reverse transcription with polymerase chain reaction (RT–PCR) from human brain or heart total RNA, followed by subcloning into the appropriate expression vectors (see below). The DNA sequence of the insert as well as the flanking regions in each cDNA clone was verified by sequencing. Numbers in the designated ALS2 clones correspond to the encoded amino acids of the ALS2 or EEA1 protein. Mutant constructs harboring point mutations were generated by oligonucleotide-directed mutagenesis using GeneEditor™ *in vitro* Site-Directed Mutagenesis System (Promega) according to the manufacturer's instructions.

ALS2 construct for antibody generation. The RLD region, encoding amino acids 1–680, was subcloned into pRSET Bacterial Expression Vector (Invitrogen), generating pRSETHis-ALS2_1–680.

ALS2 and Rabex-5 constructs for GDP/GTP exchange and in vitro *binding assays.* A total of eight cDNA fragments (one encoding full-length *ALS2*, six encoding truncated *ALS2* fragments and one encoding *RABEX5*) were subcloned into the modified pCI-neo Mammalian Expression Vector (Promega), allowing the production of amino-terminally FLAG-tagged proteins. Constructs were as follows: pCIneoFLAG–ALS2_L (full-length); pCIneoFLAG–ALS2_660–1657, pCIneoFLAG–ALS2_913–1657; pCIneoFLAG–ALS2_1018–1657; pCIneoFLAG–ALS2_1251–1657; pCIneoFLAG–ALS2_1351–1657; pCIneoFLAG–ALS2_1–1275; and pCIneoFLAG–Rabex5. Finally, two

constructs harboring different point mutations were generated: pCIneoFLAG–ALS2_660–1657(P1603A) and pCIneoFLAG–ALS2_660–1657(L1617A).

ALS2 constructs for in vitro *GST-pull down assay.* Three fragments of the *ALS2* cDNA were subcloned into pGEX–6P (Amersham Pharmacia) Bacterial expression vector, generating pGEX6P–ALS2_1018–1657, pGEX6P–ALS2_1251–1657 and pGEX6P–ALS2_1351–1657.

Small GTPase constructs for GDP/GTP exchange and in vitro *binding assays.* A total of 14 cDNA fragments encoding 14 different small GTPases, including ARF1, ARF6, Rab3A, Rab4A, Rab5A, Rab5B, Rab5C, Rab7, Rab9A, Rab11A, Ran, Rac1, RhoA and Cdc42, were subcloned into pGEX-6P bacterial expression vector (Amersham Pharmacia). The resulting constructs included pGEX6P–ARF1, pGEX6P–ARF6, pGEX6P–Rab3A, pGEX6P–Rab4A, pGEX6P–Rab5A, pGEX6P–Rab5B, pGEX6P–Rab5C, pGEX6P–Rab7, pGEX6P–Rab9A, pGEX6P–Rab11A, pGEX6P–Ran, pGEX6P–Rac1, pGEX6P–RhoA and pGEX6P–Cdc42.

Constructs for the localization studies. Full-length (ALS2_L), short form (ALS2_S) and four deletion fragments derived from the *ALS2* cDNA, and six small GTPases cDNA fragments, were subcloned into pCI-neo (Promega), pEGFP-C1 (Clontech) or p3XFLAG-CMV™-10 Expression Vector (Sigma), generating pCIneo–ALS2_L, pCIneo–ALS2_S, pEGFP–ALS2_L, pEGFP–ALS2_1–680, pEGFP–ALS2_660–1657, pEGFP–ALS2_1018–1657, pEGFP–ALS2_1351–1657, p3XFLAG–CMV10–Rab5A, p3XFLAG–CMV10–Rab5AQ79L, p3XFLAG–CMV10–Rab5AS34N, p3XFLAG–CMV10–Rab4A, p3XFLAG–CMV10–Rab7 and p3XFLAG–CMV10–Rab11A. To generate the EGFP–ALS2 constructs harboring a point mutation, the mutated *ALS2* inserts were excised from pCIneoFLAG–ALS2_660–1657(P1603A) and pCIneoFLAG–ALS2_660–1657(L1617A), and subcloned into pEGFP-C1 vector (Clontech), generating pEGFP–ALS2_660–1657(P1603A) and pEGFP–ALS2_660–1657(L1617A), respectively. Dominant negative EEA1 expression construct consisting of the carboxy-terminal fragment of EEA1 (p3XFLAG–CMV10–EEA1_1270–1411) was also generated.

Cell culture and transfection

HeLa and COS-7 cells were cultured in Dulbecco's modified Eagle's medium (DMEM) supplemented with 10% heat-inactivated fetal bovine serum (Invitorogen), 100 U/ml penicillin and 100 µg/ml streptpmycin. Primary neuronal cell cultures were established from cerebral cortex derived from embryos at 18 days (E18) of Sprague–Dawley rat according to the methods as previously described (60). HeLa/COS-7 cells and primary neuronal cells were transfected with plasmid constructs using the Effectene Transfection Reagent (Qiagen) and the LipofectAMINE 2000 (Invitrogen), respectively, according to the manufacturer's instructions.

Preparation of ALS2 and Rabex-5

COS-7 cells were transfected with pCIneo-FLAG constructs. Cells were lysed in TBST buffer [50 mM Tris–HCl; pH 7.4, 150 mM NaCl, 1 mM EDTA, 2% (w/v) Tween-20] for 3 h at 4°C, and centrifuged at 12 000*g* for 15 min at 4°C. Supernatants were immmunoprecipitated using EZview™ Red ANTI-FLAG® M2 Affnity Gel (Sigma) according to the manufacturer's instructions. The amino-terminally FLAG-tagged ALS2 and Rabex-5 proteins bound to gel beads were re-suspended in appropriate volumes of GEF buffer (25 mM Tris–HCl; pH 7.4, 50 mM NaCl, 20 mM $MgCl_2$, 1 mM CHAPS), and used for GDP/GTP exchange assay *in vitro*. A portion of the proteins was subjected to SDS–PAGE, followed by western blotting analysis with anti-FLAG antibody to estimate the amounts of conjugating FLAG-tagged proteins on the beads.

Purification of small GTPases

GST-fusion small GTPases and GST-fusion ALS2 proteins were expressed in *E. coli* BL21(DE3)pLys S (Novagen) transformed with each pGEX6P2 construct, and purified using the glutathione–Sepharose™ 4B beads (Amersham Pharmacia) according to the manufacturer's instructions. GST-fusion ALS2 proteins were used for *in vitro* binding assay. For small GTPases, GST-fusion proteins were further treated with PreScission protease (Amersham Pharmacia) to remove the GST moiety according to the manufacturer's recommendations. The resulting purified small GTPases were utilized in either GDP/GTP exchange assay or *in vitro* binding assay.

In vitro GDP/GTP exchange assay

[^{3}H]GDP dissociation assay. Each purified small GTPase (200 pmol) was loaded with [^{3}H]GDP (0.8 nmol; 370 Gbq/mmol; Amersham Pharmacia) in GXP loading buffer (25 mM Tris–HCl; pH 7.5, 50 mM NaCl, 10 mM EDTA, 5 mM $MgCl_2$, 1 mM DTT, 1 mM CHAPS) for 30 min at 30°C. To stabilize nucleotide binding, $MgCl_2$ was added to a final concentration of 20 mM, and the mixture cooled to 4°C. The GDP-loaded proteins were then purified by PD-10 column (Amersham Pharmacia) in GEF buffer. Four picomoles of the [^{3}H]GDP loaded small GTPase were pre-incubated for 5 min at 30°C, and nucleotide dissociation reaction was initiated by the addition of gel beads conjugating 2 pmol equivalent of the immunoprecipitated FLAG-tagged ALS2 or Rabex-5 protein, and further incubated for the indicated durations of time at 30°C in a final volume of 40 µl GEF buffer in the presence of 5 mM GTP. Reactions were then terminated by adding excess volume of ice-cold STOP buffer (25 mM Tris–HCl; pH 7.5, 100 mM NaCl, 20 mM $MgCl_2$), and filtered through BA85 nitrocellurose filters (Schleicher & Schell). The radioactivity trapped on the filters was counted.

[^{35}S]GTPγS binding assay. Rab5A was preloaded with either GTPγS or GDP essentially in the same manner as above. Gel beads conjugating 2 pmol equivalent of the immunoprecipitated FLAG-tagged ALS2 protein and 0.5 pmol of [^{35}S]GTPγS (37 Tbq/mmol; Amersham Pharmacia) were pre-incubated for 5 min at 30°C. Reactions were initiated by the addition of

4 pmol of Rab5A–GDP, Rab5A–GTPγS, or nucleotide-free Rab5A, and incubated for the indicated duration of time at 30°C in a final volume of 40 µl GEF buffer. Reactions were then terminated and filtered, followed by scintillation counting.

In vitro binding assay

Purified Rab5A (4 pmol), which was pre-loaded with either GDP or GTPγS, or nucleotide-free, was mixed with FLAG-M2 beads conjugating 4 pmol equivalent of the immunoprecipitated FLAG-tagged ALS2 in 100 µl of GEF buffer containing 0.1% skimmed milk for 2 h at 30°C. After washing with 4 × 1 ml of GEF buffer, the bound Rab5A was co-eluted with FLAG-ALS2 protein by the addition of SDS–PAGE sample buffer, and detected by western blotting analysis using appropriate antibodies. For GST pull-down experiments, purified small GTPases (0.3 pmol), Rab4A, Rab5A and Rab11A, which were pre-loaded with either GDP or GTPγS, or nucleotide-free, were mixed with glutathione–Sepharose 4B beads coated with 10 pmol of GST, GST–ALS2_1018–1657, GST–ALS2_1251–1657, or GST–ALS2_1351–1657 in 1 ml of binding buffer (20 mM HEPES; pH 7.4, 50 mM NaCl, 10 mM $MgCl_2$, 1 mM DTT, 0.05% Triton X-100, 100 µM GDP or GTPγS) for 1.5 h at 25°C. After washing with 4 × 1 ml of washing buffer (20 mM HEPES; pH 7.4, 100 mM NaCl, 10 mM $MgCl_2$, 1 mM DTT, 0.05% Triton X-100, 10 µM GDP or GTPγS), the bound small GTPases were co-eluted with GST fusion proteins by the addition of SDS–PAGE sample buffer, and detected by western blotting analysis using appropriate antibodies.

Immunofluorescence study

The transfected cells were washed with PBS(−) twice, fixed with 4% paraformaldehyde (PFA) in PBS(−) (pH 7.5) for 30 min at room temperature, and permeabilized with 0.5% (w/v) TritonX-100 in PBS(−) for 30 min. The primary antibodies, diluted in PBS(−) containing 1.5% normal goat serum and 0.05% TritonX-100, were added to cells and incubated for 2 h at room temperature. Alexa 594-conjugated goat anti-mouse IgG (1:200; Molecular Probes) or Alexa 594-conjugated goat anti-rabbit IgG (1:500; Molecular Probes) was used for the detection of the signals of either the tag epitope or proteins of interest. In neuronal cultured cells, ALS2 was detected by probing with anti-ALS2 polyclonal antibody (HPF1-680) and Alexa 488-conjugated anti-rabbit IgG (1:500; Molecular Probes), while Tau was visualized by staining with anti-Tau monoclonal antibody, followed by Alexa 594-conjugated goat anti-mouse IgG (1:200; Molecular Probes).

Uptake of endocytic tracers

For labeling with transferrin, HeLa cells were washed with PBS(−) twice and incubated in serum-free medium for 30 min at 37°C in 5% CO_2, followed by the incubation with serum-free medium containing 25 µg/ml transferrin Alexa 594 conjugates (Molecular Probes) for an additional 30 min at 37°C. Then, the cells were rapidly chilled with ice-cold PBS(−) and fixed with 4% PFA. For labeling with epidermal growth factor (EGF), HeLa cells were incubated with serum-free medium containing 1% BSA for 30 min at 37°C, and then incubated with fresh serum free medium containing 2.5 µg/ml EGF-tetramedtylrhodamine conjugates (Molecular Probes) for additional 30 min at 37°C. After labeling, the cells were washed and fixed in the same manner as used in transferrin labeling.

Light and confocal microscopies

Images of serial optical sections with 1–2.5 µm thickness were captured and analyzed by Leica TCS_NT confocal-microscope systems (Leica).

Immunohistochemistry

Formalin-fixed human brain samples were embedded in paraffin, and sectioned with 7 µm thickness for immunohistochemistry. Immunostaining for the ALS2 protein was performed with the affinity-purified anti-ALS2_RLD polyclonal antibody (HPF1–680) using a Vectastain elite ABC kit (Vector Lab) according to the manufacturer's recommendations.

ACKNOWLEDGEMENTS

We thank Dr A.E. MacKenzie at Ottawa University for the critical reading of the manuscript, and all the members of our laboratory for helpful discussion and suggestions. This work was founded by the Japan Science and Technology Corporation (JST) (to J.-E.I.) and the Ministry of Health, Labour and Welfare (to J.-E.I.). A part of this work was supported by a Grant-in-Aide for Scientific Research on Priority(C)—Advanced Brain Science Project from Ministry of Education, Culture, Sports, Science, and Technology, Japan (to J.-E.I.), a Grant-in-Aide for Scientific Research from Japan Society for the Promotion of Science (to S.H.), the Sumitomo Foundation (to S.H.), Kihara Memorial Yokohama Foundation for the Advancement of Life Sciences (to S.H.), and the Ichiro Kanehara Foundation (to S.H.).

REFERENCES

1. Hadano, S., Hand, C.K., Osuga, H., Yanagisawa, Y., Otomo, A., Devon, R.S., Miyamoto, N., Showguchi-Miyata, J., Okada, Y., Singaraja, R. *et al.* (2001) A gene encoding a putative GTPase regulator is mutated in familial amyotrophic lateral sclerosis 2. *Nat. Genet.*, **29**, 166–173.
2. Yang, Y., Hentati, A., Deng, H.X., Dabbagh, O., Sasaki, T., Hirano, M., Hung, W.Y., Ouahchi, K., Yan, J., Azim, A.C. *et al.* (2001) The gene encoding alsin, a protein with three guanine-nucleotide exchange factor domains, is mutated in a form of recessive amyotrophic lateral sclerosis. *Nat. Genet.*, **29**, 160–165.
3. Ben Hamida, M., Hentati, F. and Ben Hamida, C. (1990) Hereditary motor system diseases (chronic juvenile amyotrophic lateral sclerosis). *Brain*, **113**, 347–363.
4. Lerman-Sagie, T., Filiano, J., Smith, D.W. and Korson, M. (1996) Infantile onset of hereditary ascending spastic paralysis with bulbar involvement. *J. Child. Neurol.*, **11**, 54–57.
5. Eymard-Pierre, E., Lesca, G., Dollet, S., Santorelli, F.M., di Capua, M., Bertini, E., Boespflug-Tanguy, O. *et al.* (2002) Infantile-onset ascending hereditary spastic paralysis is associated with mutations in the alsin gene. *Am. J. Hum. Genet.*, **71**, 518–527.
6. Lesca, G., Eymard-Pierre, E., Santorelli, F.M., Cusmai. R., Di Capua, M., Valente, E.M., Attia-Sobol, J., Plauchu, H., Leuzzi, V., Ponzone, A. *et al.* (2003) Infantile ascending hereditary spastic paralysis (IAHSP): Clinical features in 11 families. *Neurology*, **60**, 674–682.

7. Gros-Louis, F., Meijer, I.A., Hand, C.K., Dube, M.P., MacGregor, D.L., Seni, M.H., Devon, R.S., Hayden, M.R., Andermann, F., Andermann, E. *et al.* (2003) An *ALS2* gene mutation causes hereditary spastic paraplegia in a Pakistani kindred. *Ann. Neurol.*, **53**, 144–145.
8. Leavitt, B.R. and Brunham, L.R. (2002) Hereditary motor neuron disease caused by mutations in the ALS2 gene: the long and the short of it. *Clin. Genet.*, **62**, 265–269.
9. Ohtsubo, M., Kai, R., Furuno, N., Sekiguchi, T., Sekiguchi, M., Hayashida, H., Kuma, K., Miyata, T., Fukushige, S. Murotsu, T. *et al.* (1987) Isolation and characterization of the active cDNA of the human cell cycle gene (RCC1) involved in the regulation of onset of chromosome condensation. *Genes Dev.*, **1**, 585–593.
10. Rosa, J.L. Casaroli-Marano, R.P., Buckler, A.J. Vilaró, S. and Barbacid, M. (1996) p532, a giant protein related to the chromosome condensation regulator RCC1, stimulates guanine nucleotide exchange on ARF1 and Rab proteins. *EMBO J.*, **15**, 4262–4273.
11. Schmidt, A. and Hall, A. (2002) Guanine nucleotide exchange factors for Rho GTPases: turning on the switch. *Genes Dev.*, **16**, 1587–1609.
12. Burd, C.G., Mustol, P.A., Schu, P.V. and Emr, S.D. (1996) A yeast protein related to a mammalian Ras-binding protein, Vps9p, is required for localization of vacuolar proteins. *Mol. Cell. Biol.*, **16**, 2369–2377.
13. Horiuchi, H., Lippe, R., McBride, H.M., Rubino, M., Woodman, P., Stenmark, H., Rybin, V., Wilm, M., Ashman, K., Mann, M. *et al.* (1997) A novel Rab5 GDP/GTP exchange factor complexed to Rabaptin-5 links nucleotide exchange to effector recruitment and function. *Cell*, **90**, 1149–1159.
14. Han, L., Wong, D., Dhaka, A., Afar, D., White, M., Xie, W., Herschman, H., Witte, O. and Colicelli, J. (1997) Protein binding and signaling properties of RIN1 suggest a unique effector function. *Proc. Natl Acad. Sci. USA*, **94**, 4954–4959.
15. Tall, G.G., Barbieri, M.A., Stahl, P.D. and Horazdovsky, B.F. (2001) Ras-activated endocytosis is mediated by the Rab5 guanine nucleotide exchange activity of RIN1. *Dev. Cell*, **1**, 73–82.
16. Saito, K., Murai, J., Kajiho, H., Kontani, K., Kurosu, H. and Katada, T. (2002) A novel binding protein composed of homophilic tetramer exhibits unique properties for the small GTPase Rab5. *J. Biol. Chem.*, **277**, 3412–3418.
17. Takeshima, H., Komazaki, S., Nishi, M., Iino, M. and Kangawa, K. (2000) Junctophilins: a novel family of junctional membrane complex proteins. *Mol. Cell*, **6**, 11–22.
18. Dasso, M. (2001) Running on Ran: nuclear transport and the mitotic spindle. *Cell*, **104**, 321–324.
19. Etienne-Manneville, S. and Hall, A. (2002) Rho GTPases in cell biology. *Nature*, **420**, 629–635.
20. Van Aelst, L. and Symons, M. (2002) Role of Rho family GTPases in epithelial morphogenesis. *Genes Dev.*, **16**, 1032–1054.
21. Snider, W.D., Zhou, F.-Q., Zhong, Z. and Markus, A. (2002) Signaling the pathway to regeneration. *Neuron*, **35**, 13–16.
22. Luo, L. (2000) Rho GTPases in neuronal morphogenesis. *Nat. Rev. Neurosci.*, **1**, 173–180.
23. Da Silva, J.S. and Dotti, C.G. (2002) Breaking the neuronal sphere: regulation of the actin cytoskeleton in neuritogenesis. *Nat. Rev. Neurosci.*, **3**, 694–704.
24. Zerial, M. and McBride, H. (2001) Rab proteins as membrane organizers. *Nat. Rev. Mol. Cell Biol.*, **2**, 107–117.
25. Vetter, I.R. and Wittinghofer, A. (2001) The guanine-nucleotide-binding switch in three dimensions. *Science*, **294**, 1299–1304.
26. Jensen, R.B., La Cour, T., Albrethsen, J., Nielsen, M. and Skriver, K. (2001) FYVE zinc-finger proteins in the plant model *Arabidopsis thaliana*: identification of PtdIns3*P*-binding residues by comparison of classic and variant FYVE domains. *Biochem. J.*, **359**, 165–173.
27. Mu, F.T., Callaghan, J.M., Steele-Mortimer, O., Stenmark, H., Parton, R.G,. Campbell, P.L., McCluskey, J., Yeo, J.P., Tock, E.P., Toh, B.H. *et al.* (1995) EEA1, an early endosome-associated protein: EEA1 is a conserved alpha-helical peripheral membrane protein flanked by cysteine 'fingers' and contains a calmodulin-binding IQ motif. *J. Biol. Chem.*, **270**, 13503–13511.
28. Christoforidis, S., McBride, H.M., Burgoyne, R.D. and Zerial, M. (1999) The Rab5 effector EEA1 is a core component of endosome docking. *Nature*, **397**, 621–625.
29. Wilson, J.M., de Hoop, M., Zorzi, N., Toh, B.-H., Dotti, C.G. and Parton, R.G. (2000) EEA1, a tethering protein of the early sorting endosome, shows a polarized distribution in hippocampal neurons, epithelial cells, and fibroblasts. *Mol. Biol. Cell*, **11**, 2657–2671.
30. Stenmark, H., Parton, R.G., Steele-Mortimer, O., Lutcke, A., Gruenberg, J. and Zerial, M. (1994) Inhibition of rab5 GTPase activity stimulates membrane fusion in endocytosis. *EMBO J.*, **13**, 1287–1296.
31. Sönnichsen, B., De Renzis, S., Nielsen, E., Rietdorf, J. and Zerial, M. (2000) Distinct membrane domains on endosomes in the recycling pathway visualized by multicolor imaging of Rab4, Rab5, and Rab11. *J. Cell Biol.*, **149**, 901–913.
32. Bucci, C., Parton, R.G., Mather, I.H., Stunnenberg, H., Simons, K., Hoflack, B. and Zerial, M. (1992) The small GTPase rab5 functions as a regulatory factor in the early endocytic pathway. *Cell*, **70**, 715–728.
33. Bottger, G., Nagelkerken, B. and van der Sluijs, P. (1996) Rab4 and Rab7 define distinct nonoverlapping endosomal compartments. *J. Biol. Chem.*, **271**, 29191–29197.
34. Bucci, C., Thomsen, P., Nicoziani, P., McCarthy, J. and van Deurs, B. (2000) Rab7: a key to lysosome biogenesis. *Mol. Biol. Cell*, **11**, 467–480.
35. Ullrich, O., Reinsch, S., Urbe, S., Zerial, M. and Parton, R.G. (1996) Rab11 regulates recycling through the pericentriolar recycling endosome. *J. Cell. Biol.*, **135**, 913–924.
36. Barr, F.A., Nakamura, N. and Warren, G. (1998) Mapping the interaction between GRASP65 and GM130, components of a protein complex involved in the stacking of Golgi cisternae. *EMBO J.*, **17**, 3258–3268.
37. Fukuda, M. (1994) Biogenesis of the lysosomal membrane. *Subcell. Biochem.*, **22**, 199–230.
38. Howe, C.L., Granger, B.L., Hull, M., Green, S.A., Gabel, C.A., Helenius, A. and Mellman, I. (1988) Derived protein sequence, oligosaccharides, and membrane insertion of the 120-kDa lysosomal membrane glycoprotein (lgp120): identification of a highly conserved family of lysosomal membrane glycoproteins. *Proc. Natl Acad. Sci. USA*, **85**, 7577–7581.
39. Rosenfeld, J.L., Moore, R.H., Zimmer, K.P., Alpizar-Foster, E., Dai, W., Zarka, M.N. and Knoll, B.J. (2001) Lysosome proteins are redistributed during expression of a GTP-hydrolysis-defective rab5a. *J. Cell Sci.*, **114**, 4499–4508.
40. Lawe, D.C., Patki, V., Heller-Harrison, R., Lambright, D. and Corvera, S. (2000) The FYVE domain of early endosome antigen 1 is required for both phosphatidylinositol 3-phosphate and Rab5 binding. Critical role of this dual interaction for endosomal localization. *J. Biol. Chem.*, **275**, 3699–3705.
41. Simonsen, A., Lippe, R., Christoforidis, S., Gaullier, J.M., Brech, A., Callaghan, J., Toh, B.H., Murphy, C., Zerial, M., Stenmark, H. *et al.* (1998) EEA1 links PI(3)K function to Rab5 regulation of endosome fusion. *Nature*, **394**, 494–498.
42. Lippé, R., Miaczynska, M., Rybin, V., Runge, A. and Zerial, M. (2001) Functional synergy between Rab5 effector Rabaptin-5 and exchange factor Rabex-5 when physically associated in a complex. *Mol. Biol. Cell*, **12**, 2219–2228.
43. Katzmann, D.J., Odorizzi, G. and Emr, S.D. (2002) Receptor down-regulation and multivesicular-body sorting. *Nat. Rev. Mol. Cell Biol.*, **3**, 893–905.
44. De Renzis, D., Sönnichsen, B. and Zerial, M. (2002) Divalent Rab effectors regulate the sub-compartmental organization and sorting of early endosomes. *Nat. Cell Biol.*, **4**, 124–133.
45. Gruenberg, J. (2001) The endocytic pathway: a mosaic of domains. *Nat. Rev. Mol. Cell Biol.*, **2**, 721–730.
46. Pfeffer, S.R., Dirac-Svejstrup, A.B. and Soldati, T. (1995) Rab GDP dissociation inhibitor: putting Rab GTPases in the right place. *J. Biol. Chem.*, **270**, 17057–17059.
47. McBride, H.M., Rybin, V., Murphy, C., Giner, A., Teasdale, R. and Zerial, M. (1999) Oligomeric complexes link Rab5 effectors with NSF and drive membrane fusion via interactions between EEA1 and Syntaxin 13. *Cell*, **98**, 377–386.
48. Panopoulou, E., Gillooly, D.J., Wrana, J.L., Zerial, M., Stenmark, H., Murphy, C. and Fotsis, T. (2002) Early endosomal regulation of Smad-dependent signaling in endothelial cells. *J. Biol. Chem.*, **277**, 18046–18052.
49. Clague, M.J. and Urbé, S. (2001) The interface of receptor trafficking and signaling. *J. Cell Sci.*, **114**, 3075–3081.
50. Zhao, X., Alvarado, D., Rainier, S., Lemons, R., Hedera, P., Weber, C.H., Tukel, T., Apak, M., Heiman-Patterson, T., Ming, L. *et al.* (2001) Mutations in a newly identified GTPase gene cause autosomal dominant hereditary spastic paraplegia. *Nat. Genet.*, **29**, 326–331.
51. Hazan, J., Fonknechten, N., Mavel, D., Paternotte, C., Samson, D., Artiguenave, F., Davoine, C.S., Cruaud, C., Durr, A., Wincker, P. *et al.* (1999) Spastin, a new AAA protein, is altered in the most frequent form of autosomal dominant spastic paraplegia. *Nat. Genet.*, **23**, 296–303.

52. Reid, E., Kloos, M., Ashley-Koch, A., Hughes, L., Bevan, S., Svenson, I.K., Graham, F.L., Gaskell, P.C., Dearlove, A., Pericak-Vance, M.A. *et al.* (2002) A kinesin heavy chain (*KIF5A*) mutation in hereditary spastic paraplegia (SPG10). *Am. J. Hum. Genet.*, **71**, 1189–1194.
53. Patel, H., Cross, H., Proukakis, C., Hershberger, R., Bork, P., Ciccarelli, F.D, Patton, M.A., McKusick, V.A. and Crosby, A.H. (2002) *SPG20* is mutated in Troyer syndrome, an hereditary spastic paraplegia. *Nat. Genet.*, **31**, 347–348.
54. Brownlees, J., Ackerley, S., Grierson, A.J., Jacobsen, N.J., Shea, K., Anderton, B.H., Leigh, P.N., Shaw, C.E. and Miller, C.C. (2002) Charcot-Marie-Tooth disease neurofilament mutations disrupt neurofilament assembly and axonal transport. *Hum. Mol. Genet.*, **11**, 2837–2844.
55. Crosby, A.H. and Proukakis, C. (2002) Is the transportation highway the right road for hereditary spastic paraplegia? *Am. J. Hum. Genet.*, **71**, 1009–1016.
56. Zhao, C., Takita, J., Tanaka, Y., Setou, M., Nakagawa, T., Takeda, S., Yang, H.W., Terada, S., Nakata, T., Takei, Y. *et al.* (2001) Charcot-Marie-Tooth disease type 2A caused by mutation in a microtubule motor KIF1Bβ. *Cell*, **105**, 587–597.
57. Verhoeven, K., De Jonghe, P., Coen, K., Verpoorten, N., Auer-Grumbach, M., Kwon, J.M., FitzPatrick, D., Schmedding, E., De Vriendt, E., Jacobs, A., Van Gerwen. V. *et al.* (2003) Mutations in the small GTP-ase late endosomal protein RAB7 cause Charcot-Marie-Tooth type 2B neuropathy. *Am. J. Hum. Genet.*, **72**, 722–727.
58. Cleveland, D.W. and Rothstein, J.D. (2001) From Charcot to Lou Gehrig: deciphering selective motor neuron death in ALS. *Nat. Rev. Neurosci.*, **2**, 806–819.
59. Julien, J.-P. (2001) Amyotrophic lateral sclerosis: unfolding the toxicity of the misfolded. *Cell*, **104**, 581–591.
60. Bito, H., Furuyashiki, T., Ishihara, H., Shibasaki, Y., Ohashi, K., Mizuno, K., Maekawa, M., Ishizaki, T. and Narumiya, S. (2000) A critical role for a Rho-associated kinase, p160ROCK, in determining axon outgrowth in mammalian CNS neurons. *Neuron*, **26**, 431–441.

Single-nucleotide polymorphisms in uncoding regions of *ALS2* gene of Japanese patients with autosomal-recessive amyotrophic lateral sclerosis

Isao Nagano*, Tetsuro Murakami*, Mito Shiote*, Yasuhiro Manabe*, Shinji Hadano†, Yoshiko Yanagisawa†, Joh-E Ikeda† and Koji Abe*

*Department of Neurology, Graduate School of Medicine and Dentistry, Okayama University, Okayama
†Department of Molecular Neuroscience, The Institute of Medical Sciences, Tokai University, Kanagawa, Japan

ALS2 is an autosomal recessive form of amyotrophic lateral sclerosis (AR–ALS) with juvenile onset, and has been mostly found in North African and Middle Eastern countries. Deletion mutations in the coding exons of a new gene ALS2, *encoding a protein with guanine–nucleotide exchange factor (GEF) domains, have recently been identified in ALS2 patients. These mutations are predicted to cause a loss of protein function, indicating that* ALS2 *is the causative gene underlying ALS2. To examine whether* ALS2 *is mutated in Japanese ALS patients sharing some characteristics of ALS2, we analyzed* ALS2 *gene from three patients with AR–ALS. While no deletion mutation was detected in the coding regions of* ALS2 *gene, several single-nucleotide polymorphisms (SNPs) that have been found in healthy controls as well as in Tunisian ALS2 patients were found mostly in intronic regions of the gene. These results suggest that deletion mutations in* ALS2 *gene detected in ALS2 patients seem to be uncommon in Japanese AR–ALS, and that SNPs in uncoding regions might possibly be relevant to predisposition to ALS.* [Neurol Res 2003; **25**: 505–509]

Keywords: ALS; ALS2; autosomal–recessive ALS; ALS2 *gene; deletion mutations; SNPs*

INTRODUCTION

ALS2 is a familial type of amyotrophic lateral sclerosis (ALS) transmitted as autosomal recessive (AR) trait, which was first found in a large inbred family from Tunisia[1,2]. Clinical features of ALS2 are characterized by early onset and slower progression of symptoms than classical ALS, with some cases showing prominent upper motor signs in the limbs and the facial and pharyngeal muscles. Two groups have independently identified deletion mutations linked to ALS2 in the coding exons of the new gene *ALS2* located on chromosome 2q33[3,4]. In these studies, *ALS2* gene has been shown to encode a protein with three guanine–nucleotide exchange factor (GEF) domains. Functional loss of this protein is presumed to be implicated in ALS2. Many single-nucleotide polymorphisms (SNPs) in intronic regions as well as coding exons in *ALS2* gene have also been detected, some of which were predicted to effect an amino acid change. Although ALS2 has not yet been found in the Japanese, mutations in *ALS2* gene would be relevant to some of Japanese patients with AR–ALS. To test this possibility, we examined *ALS2* gene of Japanese AR–ALS patients from three unrelated families.

Correspondence and reprint requests to: Isao Nagano, MD, Department of Neurology, Graduate School of Medicine and Dentistry, Okayama University, Okayama, Japan. [inagano@cc.okayama-u.ac.jp]
Accepted for publication February 2002.

MATERIALS AND METHODS

AR–ALS patients

Three Japanese families with apparent recessive transmissions of ALS were clinically examined by a team of neurologists, and the clinical information on affected individuals of these families is summarized in *Table 1*. Pedigree charts of three families are shown in *Figure 1*. Family A and Family C are consanguineous. Genomic DNA was extracted from white blood cells of patients with informed consent, and mutational analysis was performed as described below.

DNA analysis for *ALS2* gene

We have recently identified deletion mutations in the novel gene designated *ALS2* associated with one of AR–ALS, ALS2[3]. To examine whether mutations or DNA sequence alterations in the *ALS2* gene are associated with our Japanese patients, amplification of the region containing both exons and inron–exon boundaries in the *ALS2* gene was carried out. Genomic DNA (~50 ng) was

0161–6412/03/050505–05

Table 1: Clinical characteristics of three Japanese families with AR–ALS

Patient no.	Sex	Age at onset (years)	Duration of illness (years)	Spasticity	Amyotrophy	Pathological findings
1 (A, II-4)	M	45	5	+++	++	Alive
2 (A, II-2)	F	30	10	+++	++	Numerous axonal spheroids
3 (B, II-3)	M	47	3	++	++	Not available
4 (B, II-5)	M	52	13	++	++	Alive
5 (C, II-2)	F	61	9	+++	+	Alive
6 (C, II-4)	M	58	2	+++	+	Alive

Table 2: Summary of sequence polymorphisms in *ALS2* detected in Japanese AR–ALS patients

Region	Position*	Control	Case 2	Case 4	Case 6	Tunisian ALS2
Intron 2	IVS2+6	A/A	A/A	A/A	A/A	G/G
Intron 2	IVS2+7	T/C SNP	T/T	T/C	T/T	C/C
Intron 4	IVS4-27	A/G SNP	A/A	A/G	A/A	G/G
Intron 9	IVS9-213	T/C SNP	T/C	C/C	T/C	T/T
Intron 10	IVS10-62	T/C SNP	T/C	C/C	T/C	T/T
Exon 13	2466	A/G SNP	A/G	G/G	A/G	A/A
Intron 13	IVS13-133	T/C SNP	T/C	T/T	T/C	C/C
Exon 15	2796	T/C SNP	T/C	T/C	T/C	C/C
Intron 20	IVS2C-75	A/G SNP	A/A	A/G	A/A	A/A
Intron 22	IVS22-112	T/C SNP	T/T	T/T	T/T	T/T
Intron 25	IVS25-76	T/C SNP	T/C	T/T	T/C	C/C
Intron 29	IVS29+7	A/G SNP	G/G	G/A	G/G	G/G
Exon 34	5827	A/G SNP	A/G	A/A	A/A	A/A
Exon 34	5867	T/C SNP	T/C	T/C	T/C	C/C
Exon 34	5978	A/G SNP	A/G	A/G	A/G	G/G

*The nucleotide positions follow previously described rules for nomenclature[19]. IVA, intervening sequence; SNP, single-nucleotide polymorphism.

subjected to PCR amplification using ExTaq polymerase (Takara Bio Inc., Otsu, Japan) with parameters consisting of 95°C for 15 sec, 60°C for 30 sec, and 72°C for 30 sec for 35 cycles. Oligonucleotide primers for these PCR reactions were previously reported[3]. To detect DNA sequence variations in exons or intron–exon boundaries, DNA sequencing of the PCR products was performed. DNA sequences obtained from the patients and three Tunisian and one Japanese controls were compared, and the nucleotide variations were identified.

To examine possible mutations in the SOD1 gene in the ALS patients studied, five exons of SOD1 gene were amplified by PCR using genomic DNA, and DNA sequencing of the PCR products was performed as described elsewhere[5,6].

RESULTS

Two patients with ALS are present in each family (*Figure 1*). The mode of inheritance of ALS in Family A and Family C is thought to be AR because both sexes are affected, parents of the patients are always healthy, and patients are derived from consanguineous families. Family B could be AR although it might represent autosomal dominant with incomplete penetrance or X-linked inheritance. The clinical features of the patients studied in the present study are summarized in *Table 1*. No mutation in SOD1 gene has been detected in all families. Post-mortem pathological examinations of Patient 2 demonstrated numerous axonal spheroids throughout the central nervous system (*Table 1*). Similar to Tunisian and Kuwaiti ALS2, all of our Japanese AR–ALS patients exhibited marked upper motor signs in addition to amyotrophy of legs and hands. Furthermore, the duration of illness of our patients was relatively long, which is also the characteristic of ALS2. However, our patients developed disease at age 30 to 61 years, which is older than Tunisian ALS2 patients whose ages of onset ranged from 3 to 23 years[1].

All 34 exons and flanking regions of *ALS2* gene were examined as described. Although no deletion of missense mutations were found in the coding regions

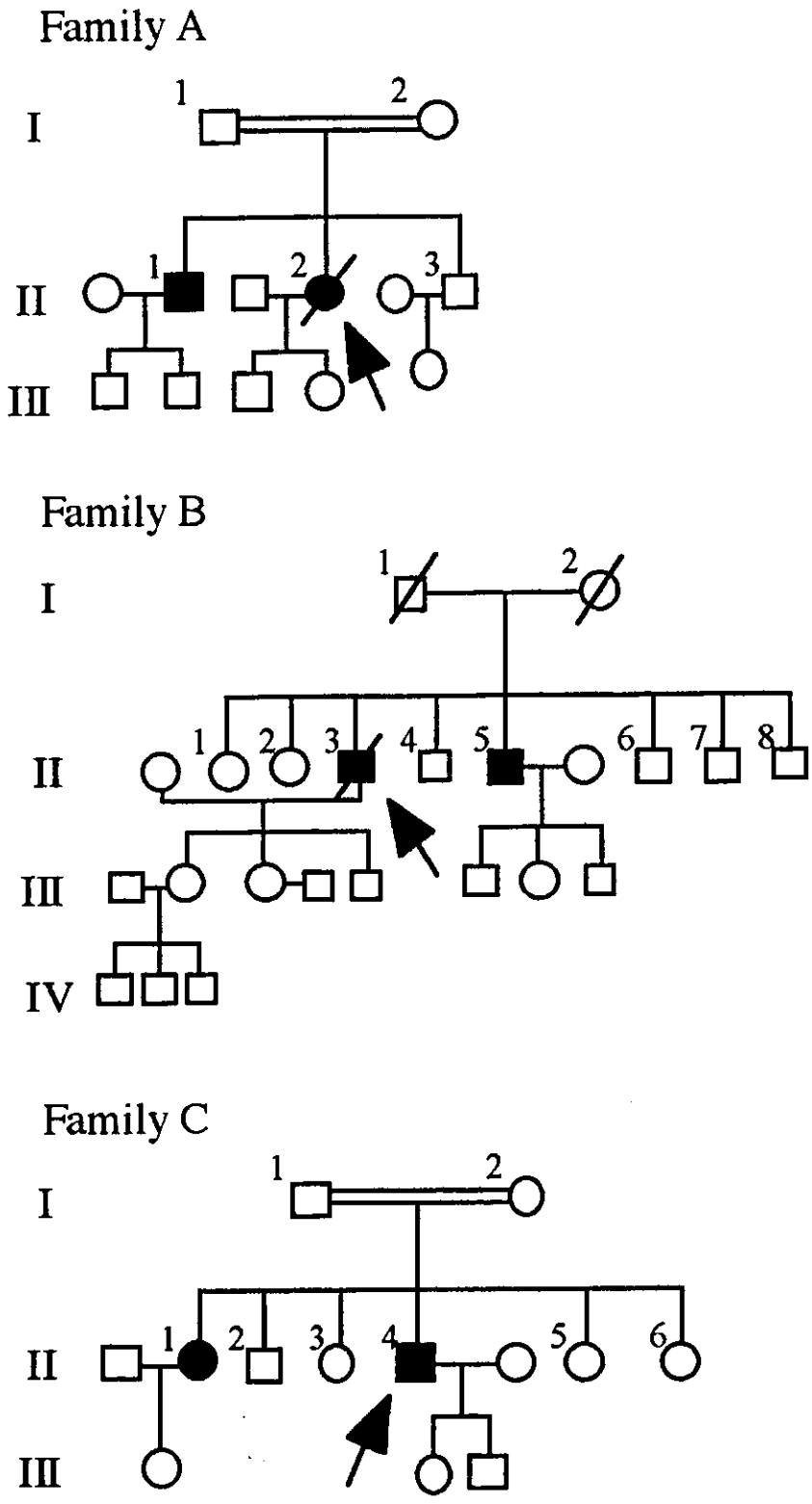

Figure 1: Pedigrees of three Japanese families affected by AR–ALS. Squares and circles indicate males and females; solid symbols, affected individuals; double horizontal lines, consanguineous marriage; slash marks, the deceased; arrows, probands

of *ALS2* gene in all patients examined, several SNPs were found mainly in intronic regions of the gene (*Table 2*). As indicated in *Table 2*, none of these SNPs were unique compared to normal controls with Tunisian and Japanese backgrounds. While six intronic sequence variations and two exonic sequence changes have been shown to be associated with Tunisian ALS2[3], the same sequence polymorphisms were not observed in our patients. Some SNPs were also detected in the coding exons 13, 15 and 34 of *ALS2* gene (*Table 2*). However, all these SNPs were found in controls as well, and none of these SNPs are predicted to effect amino acid change. As for SOD1 gene, none of the ALS patients demonstrated mutations in the coding exons of the gene.

DISCUSSION

In Tunisian and Kuwaiti ALS2 patients, a single-nucleotide deletion in exon 3 and a 2-bp deletion in exon 5 of *ALS2* gene were detected[1,4]. In addition, the Saudi family has been reported to have a 2-bp deletion in exon 9[4]. These mutations result in frameshifts that generate premature stop codons, probably causing a loss of protein function. The *ALS2* gene is expressed in neuronal cells throughout the brain and spinal cord, including spinal motor neurons[3]. Although the precise function of ALS2 remains unknown, there are three GEF domains in the protein sequence deduced for ALS2: regulator of chromosome condensation (RCC1), GEF for Rho, and vacuolar protein sorting 9 (VPS9)[3,4,7–10]. Since these GEFs are thought to be involved in microtubule assembly, membrane organization and trafficking in various cells including neurons, loss of those functions may result in defects of axonal transport and cytoskeletal organization[11,12].

In the present study, none of our AR–ALS patients exhibited mutations in the coding exons of *ALS2* gene that have been detected in Tunisian/Kuwaiti ALS2 patients. Since the identical phenotype to Tunisian/Kuwaiti ALS2 has not yet been found in Japanese ALS patients, ALS2 might be uncommon in Japanese population, and mutations in unknown gene(s) other than *ALS2* could be attributed to our AR–ALS patients. Instead, several SNPs have been found mainly in uncoding regions of *ALS2* gene in our patients, implying that *ALS2* may have additional SNPs in other uncoding regions as well. Polymorphisms, particularly in the regulatory regions of genes, potentially affect expression of the genes and may be relevant to disease susceptibility[13,14]. Although the SNPs detected in the present study may not affect the function of ALS2 protein, it is also possible that some mutations in unexamined intronic or promotor regions of the gene may influence the processing of *ALS2* and play a role as a risk factor.

The pathological analysis of Patient 2 showed conspicuous axonal spheroid formation in the spinal cord, suggesting that axonal transport is impaired at least in one of our AR–ALS families. Since others and we have observed an impairment of axonal transport in SOD1 mutant mice with remarkable axonal spheroid formation[15–18], impairment of axonal transport could be relevant to our ALS patients. Overall, mutations in *ALS2* gene observed in Tunisian/Kuwaiti ALS2 patients were not found in our Japanese AR–ALS patients, while several SNPs were detected mostly in the uncoding regions. Although the significance of these SNPs remains elusive, further studies will clarify the exact function of ALS2 protein, and whether SNPs in uncoding regions modify its function and serve as a risk factor in ALS.

ACKNOWLEDGEMENTS

This study was partly supported by a Grant-in-Aid for Scientific Research (B) 12470141 from the Ministry of Education, Culture, Sports, Science and Technology of Japan, and by grants from the Ministry of Health, Welfare and Labor of Japan.

REFERENCES

1 Ben Hamida M, Hentati F, Ben Hamida C. Hereditary motor system diseases (chronic juvenile amyotrophic lateral sclerosis). *Brain* 1990; **113**: 347–363
2 Hentati A, Begaoui K, Pericak-Vance MA, Hentati F, Speer MC, Hung WY, Figlewicz DA, Haines J, Rimmler J, Ben Hamida C, *et al.* Linkage to recessive familial amyotrophic lateral sclerosis to chromosome 2q33-q35. *Nat Genet* 1994; **7**: 425–428
3 Hadano S, Hand CK, Osuga H, Yanagisawa Y, Otomo A, Devon RS, Miyamoto N, Showguchi-Miyata J, Okada Y, Singaraja R, Figlewicz DA, Kwiatkowski T, Hosler BA, Sagie T, Skaug J, Nasir J, Brown RH Jr, Scherer SW, Rouleau GA, Hayden MR, Ikeda JE. A gene encoding a putative GTPase regulator is mutated in familial amyotrophic lateral sclerosis 2. *Nat Genet* 2001; **29**: 166–173
4 Yang Y, Hentati A, Deng HX, Dabbagh O, Sasaki T, Hirano M, Hung WY, Ouahchi K, Yan J, Azim AC, Cole N, Gascon G, Yagmour A, Ben-Hamida M, Pericak-Vance M, Hentati F, Siddique T. The gene encoding alsin, a protein with three guanine-nucleotide exchange factor domains, is mutated in a form of recessive amyotrophic lateral sclerosis. *Nat Genet* 2001; **29**: 160–165
5 Abe K, Aoki M, Ikeda M, Watanabe M, Hirai S, Itoyama Y. Clinical characteristics of familial amyotrophic lateral sclerosis with Cu/Zn superoxide dismutase gene mutations. *J Neurol Sci* 1996; **136**: 108–116
6 Watanabe M, Aoki M, Abe K, Shoji M, Iizuka T, Ikeda Y, Hirai S, Kurokawa K, Kato T, Sasaki H, Itoyama Y. A novel missense point mutation (S134N) of the Cu/Zn superoxide dismutase gene in a patient with familial motor neuron disease. *Hum Mutat* 1997; **9**: 69–71
7 Ohtsubo M, Kai R, Furuno N, Sekiguchi T, Sekiguchi M, Hayashida H, Kuma K, Miyata T, Fukushige S, Murotsu T, *et al.* Isolation and characterization of the active cDNA of the human cell cycle gene (RCC1) involved in the regulation of onset chromosome condensation. *Genes Dev* 1987; **1**: 585–593
8 Soisson SM, Nimnual AS, Uy M, Bar-Sagi D, Kuriyan J. Crystal structure of the Dbl and pleckstrin homology domains from the human Son of sevenless protein. *Cell* 1998; **95**: 259–268
9 Hama H, Tall GG, Horazdovsky BF. Vps9p is a guanine nucleotide exchange factor involved in vesicle-mediated vacuolar protein transport. *J Biol Chem* 1999; **274**: 15284–15291
10 Kahana JA, Cleveland DW. Some importin news about spindle assembly. *Science* 2001; **291**: 1718–1719
11 Collard JF, Cote F, Julien JP. Defective axonal transport in a transgenic mouse model of amyotrophic lateral sclerosis. *Nature* 1995; **375**: 61–64
12 Williamson TL, Cleveland DW. Slowing of axonal transport is a very early event in the toxicity of ALS-linked SOD1 mutants to motor neurons. *Nat Neurosci* 1999; **2**: 50–56

13 Todd JA. From genome to aetiology in a multifactorial disease, type I diabetes. *Bioessays* 1999; **21**: 164–174
14 Lambert JC, Mann DM, Harris JM, Chartier-Harlin MC, Cumming A, Coates J, Lemmon H, StClair D, Iwatsubo T, Lendon C. The −48 C/T polymorphism in the presenilin 1 promoter is associated with an increased risk of developing Alzheimer's disease and an increased Abeta load in brain. *J Med Genet* 2001; **38**: 353–355
15 Wong PC, Pardo CA, Borchelt DR, Lee MK, Copeland NG, Jenkins NA, Sisodia SS, Cleveland DW, Price DL. An adverse property of a familial ALS-linked SOD1 mutation causes motor neuron disease characterized by vacuolar degeneration of mitochondria. *Neuron* 1995; **14**: 1105–1116
16 Bruijn LI, Becher MW, Lee MK, Anderson KL, Jenkins NA, Copeland NG, Sisodia SS, Rothstein JD, Borchelt DR, Price DL, Cleveland DW. ALS-linked SOD1 mutant G85R mediates damage to astrocytes and promotes rapidly progressive disease with SOD1-containing inclusions. *Neuron* 1997; **18**: 327–338
17 Warita H, Itoyama Y, Abe K. Selective impairment of fast axonal transport in the peripheral nerves of asymptomatic transgenic mice with G93A mutant SOD1 gene. *Brain Res* 1999; **819**: 120–131
18 Murakami T, Nagano I, Hayashi T, Manabe Y, Shoji M, Setoguchi Y, Abe K. Impaired retrograde axonal transport of adenovirus-mediated *E. coli* LacZ gene in the mice carrying mutant SOD1 gene. *Neurosci Lett* 2001; **308**: 149–152
19 Dunnen JT, Antonarakis SE. Mutation nomenclature extensions and suggestions to describe complex mutations: A discussion. *Hum Mutat* 2000; **15**: 7–12

THE JOURNAL OF BIOLOGICAL CHEMISTRY
Vol. 279, No. 8, Issue of February 20, pp. 7275–7286, 2004
Printed in U.S.A.

Novel Nuclear Shuttle Proteins, HDBP1 and HDBP2, Bind to Neuronal Cell-specific *cis*-Regulatory Element in the Promoter for the Human Huntington's Disease Gene*

Received for publication, September 29, 2003, and in revised form, November 17, 2003
Published, JBC Papers in Press, November 18, 2003, DOI 10.1074/jbc.M310726200

Kazunori Tanaka‡§, Junko Shouguchi-Miyata‡, Natsuki Miyamoto§, and Joh-E Ikeda‡§¶‖

From the ‡Department of Molecular Neuroscience, Institute of Medical Sciences, Tokai University, Isehara, Kanagawa 259-1193, Japan, the §Solution Oriented Research for Science and Technology, Japan Science and Technology Corporation, Tokai University School of Medicine, Isehara, Kanagawa 259-1193, Japan, and the ¶Department of Paediatrics, Faculty of Medicine, University of Ottawa, Ottawa, Ontario K1H 8M5, Canada

Huntington's disease (HD) is a neurodegenerative disease caused by a CAG repeat expansion in exon 1 of the *HD* gene, and the expression level of either normal or mutant huntingtin is implicated in the pathogenesis of HD. However, a molecular base of the *HD* gene transcription has not been elucidated as yet. In this study, we identified two proteins, HDBP1 and HDBP2, which bind to the promoter region for the *HD* gene using a yeast one-hybrid system. Amino acid sequence analysis of the proteins deduced the presence of nuclear localization signal, nuclear export signal, zinc finger, serine/proline-rich region, and highly conserved C-terminal region. *In vitro* DNA binding assay indicated that the C-terminal conserved regions of the proteins were responsible for binding to the unique promoter DNA sequences of the *HD* gene. The DNA sequence protected from DNase I digestion was a 7-bp consensus sequence (GCCGGCG), which resides in triplicate at intervals of 13 bp within and proximal to the 20-bp direct repeat sequences of the *HD* promoter region. The mutation of 7-bp consensus sequence abolishes the *HD* promoter function in a neuronal cell line (IMR32). In human cultured cells, ectopically expressed green fluorescent protein-fused HDBP1 and HDBP2 localized in the cytoplasm, but both proteins totally shift from cytoplasm to nucleus by the treatment with an inhibitor of the nuclear export, leptomycin B, and mutagenesis of the putative nuclear export signals. Taken together, HDBP1 and HDBP2 are novel transcription factors shuttling between nucleus and cytoplasm and bind to the specific GCCGGCG, which is an essential *cis*-element for *HD* gene expression in neuronal cells.

Huntington's disease (HD)[1] is an autosomal dominant neurodegenerative disorder characterized by involuntary movements, cognitive impairment, and emotional disturbance (1). HD is caused by an expansion of the CAG trinucleotide repeat within exon 1 of the *HD* gene, which encodes a cytoplasmic protein named huntingtin (2). The number of CAG repeats is polymorphic, ranging from 6 to 35 on normal chromosomes and 36 or more on HD chromosomes. The CAG trinucleotide repeat is translated into polyglutamine (polyQ). Expression of the mutant huntingtin carrying an expanded polyQ tract induces the formation of the nuclear and cytoplasmic aggregates in the brain, as well as in peripheral tissues of HD patients (3–5). However, the question as to whether the role of the aggregates is protective or pathogenic remains to be solved.

Several lines of evidences from *in vitro* experiments as well as HD model mice suggest that a gain of toxic property acquiring in the mutant huntingtin is a major cause for HD pathogenesis. Recently, it has been shown that the expanded polyQ binds to a group of transcription factors, such as Sp1, cAMP-responsive element-binding protein-binding protein (CBP), p300/CBP-associated factors (P/CAF), and $TAF_{II}130$ (6–13), and could perturb their normal functions. This could lead to transcriptional dysregulation in a number of genes under controlling by these transcription factors, and ultimately to dysfunction of the cells. Thus, one of the possible toxic entities could be the ability of polyQ for binding to several transcription factors. To alleviate the pathology seen in HD, removing or reducing such toxic entities is one of the challenges in the development of disease therapies for HD as well as other polyQ diseases such as spinocerebellar ataxias and dentatorubral pallidoluysian atrophy. However, molecular mechanisms underlying the dysregulation of cellular systems, including the downstream signaling pathways mediated by the mutant huntingtin, remain elusive.

Several studies using animal models for HD have given important insights into the pathogenesis and cure for HD. Using YAC transgenic mice as a HD model, Leavitt *et al.* (14) have reported that normal huntingtin competes against mutated huntingtin to reduce the toxicity, suggesting that an increment of normal huntingtin could delay disease progression. On the other hand, the study of the conditional mouse

* This work was supported in part by a grant-in-aid for scientific research on priority areas (Advanced Brain Science Project) from the Ministry of Education, Culture, Sports, Science and Technology, Japan. The costs of publication of this article were defrayed in part by the payment of page charges. This article must therefore be hereby marked "*advertisement*" in accordance with 18 U.S.C. Section 1734 solely to indicate this fact.

The nucleotide sequence(s) reported in this paper has been submitted to the GenBank™/EBI Data Bank with accession number(s) AB044750, AB044786, AB052777, AB073627, and AF292939

‖ To whom correspondence should be addressed: Dept. of Molecular Neuroscience, Inst. of Medical Sciences, Tokai University, Isehara, Kanagawa 259-1193, Japan. Tel.: 81-463-91-5095; Fax: 81-463-91-4993; E-mail: joh-e@nga.med.u-tokai.ac.jp or joh-e@mgcheo.med.uottawa.ca.

[1] The abbreviations used are: HD, Huntington's disease; polyQ, polyglutamine; NLS, nuclear localization signal; NES, nuclear export signal; LMB, leptomycin B; HDBP, *HD* gene regulatory region-binding protein; CBP, cAMP-responsive element-binding protein-binding protein; P/CAF, p300/CBP-associated factors; GST, glutathione *S*-transferase; GFP, green fluorescent protein; GEFdb, GLUT4 enhancer factor DNA-binding domain; PBF, papillomavirus binding factor; GIG1, glucocorticoid-induced gene 1; ORF, open reading frame; aa, amino acid(s); CR, conserved region; UTR, untranslated region; nt, nucleotide(s); RACE, rapid amplification of cDNA ends; 3-AT, 3-aminotriazole; PIPES, 1,4-piperazinediethanesulfonic acid; EMSA, electrophoretic mobility shift assay.

model of HD using the tetracycline-responsive gene system demonstrated that a blockade of expression of mutated gene in symptomatic mice led to a disappearance of aggregates and an amelioration of the behavioral phenotypes, indicating that a continuous expression of the mutated huntingtin was required to maintain aggregate formation, as well as some symptoms, and that HD may be reversible (15). Taken together, the levels of normal and mutated huntingtin may influence severity and progression of the disease. It is feasible to intervene in the progression or even to cure the disease by means of the manipulation of the mutated and/or normal huntingtin gene expression. As a first step toward this, comprehension of the molecular basis of the *HD* transcriptional regulation should be a primary objective.

To delineate the transcriptional regulation for the *HD* gene, we must perceive: 1) the structure of the promoter region including unique *cis*-regulatory elements, 2) *trans*-acting factors that bind to these *cis*-regulatory elements, and 3) how these factors contribute to induce or suppress its expression in the cells. Thus far, several studies on the structure and/or sequences for the promoter region of the *HD* gene have been published. The *HD* promoter region consists of a GC-rich DNA sequence containing several potential binding sites for Sp1, AP2, and AP4, whereas it lacks both typical TATA and CAAT boxes (16, 17). There are two copies of the 20-bp direct repeat and two copies of the 17-bp direct repeat in the 5′ region of the *HD* gene (17). These unique repeat sequences have postulated to be *cis*-regulatory elements, which contribute to the regulation of transcription of the *HD* gene. In particular, the 20-bp direct repeat sequences are shown to be required for the enhanced transcription (18). However, no *trans*-acting factors that bind to these candidate *cis*-regulatory elements on the *HD* promoter have been identified yet, let alone understanding the molecular mechanisms by which the transcription of the *HD* gene is regulated.

To aid in the delineation of the transcriptional regulation of the *HD* gene, we sought to explore *trans*-acting factors that bound to the promoter region of the *HD* gene. We report in this study the identification of two members of a novel nuclear shuttle protein family, *HD* gene regulatory region-binding protein (HDBP) 1 and HDBP2, which are found to be an exact match of GLUT4 enhancer factor DNA binding domain (GEFdb) (19) and papillomavirus binding factor (PBF) (20), respectively. Both factors specifically bind to the triplicated 7-bp consensus sequence (GCCGGCG) at intervals of 13 bp in the *HD* promoter region. The *HD* promoter function, especially in a neuronal cell line (IMR32), relies on the 7-bp consensus sequence. These novel DNA-binding proteins in conjunction with the novel *cis*-regulatory element, GCCGGCG, can trigger off *HD* gene transcription in a neuronal cell line. These elements provide new clues to the understanding of the transcriptional regulation of the *HD* gene in neuron.

EXPERIMENTAL PROCEDURES

Reagent—Nuclear export signal (NES) inhibitor leptomycin B (LMB) (21, 22) was a gift from Dr. Minoru Yoshida (University of Tokyo, Tokyo, Japan).

Yeast One-hybrid Screening—The Matchmaker one-hybrid system (Clontech) was used to isolate cDNA clones encoding DNA-binding factor for the promoter region of the *HD* gene. A plasmid DNA containing 2.0 kilobase pairs of 5′-flanking region of the *HD* gene with $(CAG)_{18}$ (23) was used as a template for the PCR amplification. To generate target reporter construct for library screening, the DNA fragment containing the 5′-flanking region and a portion of exon 1 of the *HD* gene, corresponding with the nucleotide sequences from −365 to +158, was amplified by PCR using the primer pair 5′-GTTGAGCCCCGCGCCTTCG-3′ and 5′-GGCTGAGGAAGCTGAGGAG-3′. The amplified fragment was inserted into the SmaI sites of pHISi-1 and pHISi reporter vectors, resulting in target-reporter constructs, pHISi-1-R1-2-3-4 and pHISi-R1-2-3-4, respectively. Yeast transformants containing either pHISi-1-R1-2-3-4 or pHISi-R1-2-3-4 reporter construct were established by transforming a yeast YM4271 strain with XhoI-linearized pHISi-1-R1-2-3-4 or pHISi-R1-2-3-4, followed by the selection on the SD/−His medium. Then, human testis Matchmaker cDNA (GAL4 activation domain) library (pACT2 library) was introduced into these reporter strains. Transformants growing on SD/−His/−Leu medium containing 45 mM 3-aminotriazole (3-AT) were isolated as positive clones (pACT2 clones), encoding the DNA-binding protein. Isolation of cDNA from yeast transformants was performed according to the protocol from the manufacturer (Clontech).

To confirm DNA binding activity and its specificity among the positive clones, additional reporter strains carrying smaller DNA fragments, R1 (−365 to −214), R2 (−231 to −113), R3 (−131 to +51), and R4 (+29 to +158), were generated by PCR amplification using the primer pairs 5′-AAAGAATTCGTTGAGCCCCGCGCCTTCG-3′/5′-AAATGCGCAACGCCGGCCAGCATGATT-3′, 5′-AAAGAATTCAATCATGCTGGCCGGCGT-3′/5′-AAATGCGCAAGCGGCCGTCCATCTTGGA-3′, 5′-AAAGAATTCTCCAAGATGGACGGCCGCT-3′/5′-AAATGCGCAGAAGGACTTGAGGGACTCGAAGG-3′, and 5′-AAAGAATTCCCTTCGAGTCCCTCAAGTCCTTC-3′/5′-AAATGCGCAGGCTGAGGAAGCTGAGGAG-3′, respectively. Each amplified fragment was digested with EcoRI and MluI and inserted into both pHISi-1 and pHISi reporter vectors, resulting in eight target-reporter constructs, pHISi-1-R1, pHISi-R1, pHISi-1-R2, pHISi-R2, pHISi-1-R3, pHISi-R3, pHISi-1-R4, and pHISi-R4. Reporter strains were established by transforming a yeast YM4271 strain with XhoI-linearized constructs, followed by the selection on the SD/−His medium plate. After re-transformation of each reporter strain with the positive cDNA (pACT2 clone) clone, the DNA-protein interaction was assayed by the growth of transformants on the SD/−His/−Leu medium plate containing 45 mM 3-AT.

Isolation of the Entire Coding Sequence of Transcripts—To isolate full-length cDNA for HDBP1, 1.5×10^5 plaque-forming units of the human testis cDNA library (insert size: larger than 0.5 kb) was screened by the standard procedure (Stratagene). In brief, phage plaques were plated, lifted and fixed onto nylon filters, and hybridized with the ^{32}P-labeled 1.3-kb HDBP1 cDNA fragment for 18 h in hybridization solution (2× PIPES buffer, 50% deionized formamide, 0.5% SDS, 100 μg/ml herring testis) at 42 °C. The filters were washed twice for 5 min in 2× SSC at room temperature and for 30 min in 0.1× SSC, 0.1% SDS at 55 °C. Autoradiography was performed for 1–2 days using x-ray film (Eastman Kodak Co., BioMax) at −80 °C. The resulting positive phage clone was converted into plasmid DNA (pBluescript II; pBs) by *in vivo* excision (Stratagene), resulting in pBs-HDBP1.

To obtain the most 5′ sequence of the HDBP2 transcript, rapid amplification of cDNA ends (RACE) was performed using SMART™ RACE cDNA amplification (Clontech). First strand cDNA was synthesized from the human testis mRNA using 5′-RACE cDNA synthesis primer. Twenty-five cycles of 5′-RACE and nested PCR reactions (94 °C for 30 s; 68 °C for 3 min) were carried out using 5′-ACCCCCGTACCACACATAAACCTTC-3′ and an universal primer mix (Clontech), and 5′-GGTGCTGGGAGCCTTAAGGACT-3′ and a nested universal primer (Clontech), respectively. The 350-bp PCR product was cloned using TA cloning system (Invitrogen). The fragment containing the entire open reading frame (ORF) of HDBP2 was generated from pACT2 clone 8 by PCR using primers c8ATG (5′-AAAGAATTCATGGCGAGTGTCCTGTCCCGACGCCTTGGAAAGCGGTCCCTCCTGGGAGCCCGGGTGTTGGGACCCAGTGCCT-3′) (initiation ATG is underscored) and c8stop (5′-AAAGTCGACTCAGTCCAGAAAGCGCTG-3′). The PCR fragment was digested with EcoRI and SalI and inserted into the EcoRI-SalI site of pBs vector, resulting in pBs-HDBP2.

cDNA Sequencing and Sequence Analysis—DNA sequence of the cDNA clones was determined using a DyeDeoxy Terminator Cycle Sequencing kit and ABI377 DNA sequencer (ABI). The cDNA and predicted amino acid sequences were compared with non-redundant nucleotide and protein sequence data base using BLASTN and BLASTP (blast.genome.ad.jp/) (35), respectively. The multiple protein sequence alignment was performed using GENETYX-MAC.

Northern Blot Analysis—The filters of Gene Hunter I, II, III, and IV (non-normalized) (Toyobo) were used for Northern blot analysis. The 1.3-kb HDBP1 cDNA, the 1.7-kb HDBP2 cDNA, and the full-length β-actin cDNA were labeled with [α-^{32}P]dCTP by a random priming method. Hybridization with each labeled probe was carried out in a solution (0.5 M sodium phosphate (pH 7.2), 7% SDS, 1 mM EDTA) for 18 h at 65 °C. Filters were washed once for 5 min in 2× SSC at room temperature and for 30 min in 2× SSC, 1% SDS at 65 °C. Autoradiography was performed for 1–2 days using x-ray film (Kodak BioMax) at −80 °C.

Generation of the Plasmid Constructs—Expression constructs for

TABLE I

The list of HDBP1- and HDBP2-specific primers, vectors, and template DNAs used for PCR amplification

Plasmid DNA	vector	template DNA	primer	sequence
<GST-fusion>				
1:pGST-HDBP1	pGEX-5X-2	pBs-HDBP1	hdrf1F(*EcoRI site* Start)	5′-AAAAGAATTCGAATGGAGCGCCCCCCGCCC-3′
			hdrf1R(*XhoI site* Stop)	5′-AAAACTCGAGCTAGTCCAGGAACCGCTGGC-3′
2:pGST-HDBP1-N	pGEX-5X-2	pBs-HDBP1	hdrf1F(*EcoRI site* Start)	5′-AAAAGAATTCGAATGGAGCGCCCCCGCCC-3′
			hdrf1nR(*XhoI site* Stop)	5′-AAACTCGAGTCAGACCTCGTCCAGCCGGCTTTT-3′
3:pGST-HDBP1-Zn	pGEX-5X-2	pBs-HDBP1	hdrf1znF(*EcoRI site*)	5′-AAAGAATTCTGATGGCTGCTGCTGCCCTTACAA-3′
			hdrf1znR(*XhoI site* Stop)	5′-AAACTCGAGTCAGCCCTGGTAGACACGGTCACTGT-3′
4:pGST-HDBP1-C	pGEX-5X-1	pBs-HDBP1	hdrf1cF(*EcoRI site*)	5′-AAAGAATTCTGCCTGAAGCCCGCCCGCCTGGA-3′
			hdrf1R(*XhoI site* Stop)	5′-AAACTCGAGTTAGTCCAGGAACCGCTGGC-3′
5:pGST-HDBP1-CR3	pGEX-5X-1	pBs-HDBP1	hdrf1c1F(*EcoRI site*)	5′-AAAGAATTCAGGAAGCCCGGGGCGAGGC-3′
			hdrf1R(*XhoI site* Stop)	5′-AAAACTCGAGTTAGTCCAGGAACCGCTGGC-3′
6:pGST-HDBP2	pGEX-5X-2	pBs-HDBP2	hdrf2F(*EcoRI site* Start)	5′-AAAGAATTCTGATGGTGAGTGTCCTGTCCCGACGCCTGGAAA-3′
			hdrf2R(*XhoI site* Stop)	5′-AAACTCGAGTCAGTCCAGAAAGCCCTGCA-3′
7:pGST-HDBP2-N	pGEX-5X-2	pBs-HDBP2	hdrf2F(*EcoRI site* Start)	5′-AAAGAATTCTGATGGGAGTGTCCTGTCCCGACGCCTTGGAAA-3′
			hdrf2nR(*XhoI site* Stop)	5′-AAACTCGAGTCACATCTCATCCATTTCCACTGCGTC-3′
8:pGST-HDBP2-Zn	pGEX-5X-1	pBs-HDBP2	hdrf2znF(*EcoRI site*)	5′-AAAGAATTCATGGGCGCCATGGTGCTGACGT-3′
			hdrf2znR(*XhoI site* Stop)	5′-AAACTCGAGTCAGCGGCGGAGGGGCAGCAGCCCAGCTGACACT-3′
9:pGST-HDBP2-C	pGEX-5X-1	pBs-HDBP2	hdrf2cF(*EcoRI site*)	5′-AAAGAATTCTGCTCTCTCTCTCTGGTCCGGA-3′
			hdrf2R(*XhoI site* Stop)	5′-AAAACTCGAGTTAGTCCAGGAACCGCTGGC-3′
10:pGST-HDBP2-CR3	pGEX-5X-1	pBs-HDBP2	hdrf1c1F(*EcoRI site*)	5′-AAAGAATTCAGGAAGCCCGAGGAGGAGCT-3′
			hdrf1R(*XhoI site* Stop)	5′-AAAACTCGAGTTAGTCCAGGAACCGCTGGC-3′
<GFP-fusion>				
11:pHDBP1-GFP	pEGFP-N1	pBs-HDBP1	hdrf1gF(*EcoRI site* Start)	5′-AAAGAATTCCCACCATGGAGCGCCCCCCGCCC-3′
			hdrf1gR(*SalI site*)	5′-TTTGTCGACTGGTCCAGGAACCGCTGGCCAGGCTTT-3′
12:pHDBP1 -N-terminal-GFP	pEGFP-N1	pBs-HDBP1	hdrf1gF(*EcoRI site* Start)	5′-AAAGAATTCCCACCATGGAGCGCCCCCGCCC-3′
			hdrf1ngR(*SalI site*)	5′-AAAGTCGACTGGACCTGGGCCGGCTCTTCCTTTTT-3′
13:pHDBP1 -C-terminal-GFP	pEGFP-N1	pBs-HDBP1	hdrf1cgF(*EcoRI site* Start)	5′-AAAGAATTCCCACCATGTTCCAGTGTCTGT-3′
			hdrf1gR(*SalI site*)	5′-TTTGTCGACTGGTCCAGGAACCGCTGGCCAGGCTTT-3′
14:pHDBP2-GFP	pEGFP-N1	pBs-HDBP2	hdrf2gF(*EcoRI site* Start)	5′-AAAGAATTCCCACCATGGCGAGTGTCCTGTCCCGACGCCTTGGAAA-3′
			hdrf2gR(*SalI site*)	5′-TTTGTCGACTGGTCCAGAAAGCGCTGGCAGGCCTT-3′
15:pHDBP2 -N-terminal-GFP	pEGFP-N1	pBs-HDBP2	hdrf2gF(*EcoRI site* Start)	5′-AAAGAATTCCCACCATGGCGAGTGTCCTGTCCCGACGCCTTGGAAA-3′
			hdrf2ngR(*SalI site*)	5′-AAAGTCGACTGCATCTCATCCATTTCCACTGCGTC-3′
16:pHDBP2 -C-terminal-GFP	pEGFP-N1	pBs-HDBP2	hdrf2cgF(*EcoRI site* Start)	5′-AAAGAATTCCCACCATGCGGCCATGGTGCTGACGT-3
			hdrf2gR(*SalI site*)	5′-TTTGTCGACTGGTCCAGAAAGCGCTGGCAGGCCTT-3′
<MycHis-fusion>				
17:pHDBP1-MycHis	pcDNA3.1 -MycHisC	pBs-HDBP1	hdrf1gF(*EcoRI site* Start)	5′-AAAGAATTCCCACCATGGAGCGCCCCCGCCC-3′
			hdrf1nhR(*XhoI site*)	5′-TTTCTCGAGCGTCCAGGAACCGCTGGCCAGGCTTT-3′
18:pHDBP2-MycHis	pcDNA3.1 -MycHisC	pBs-HDBP2	hdrf2gF(*EcoRI site* Start)	5′-AAAGAATTCCCACCATGGCGAGTGTCCTGTCCCGACGCCTTGGAAA-3′
			hdrf2nhR(*XhoI site*)	5′-TTTCTCGAGCGTCCAGAAAGCGCTGGCAGGCCTT-3′

HDBP1 and HDBP2 as glutathione *S*-transferase (GST)-, green fluorescent protein (GFP)-, and MycHis-tagged fusion proteins were generated as follows. Template plasmid DNA (10 ng) was subjected to 25 cycles of PCR amplification (30 s at 94 °C and 3 min at 68 °C) using KOD polymerase (Toyobo) and primers (Table I). Each fragment was digested with EcoRI and XhoI (GST-fused HDBPs and MycHis-tagged fused HDBPs) or EcoRI and SalI (GFP-fused HDBPs) and inserted into the EcoRI-XhoI site of pGEX-5X-1 or -5X-2 (Amersham Biosciences) and pcDNA3.1-MycHisC (Clontech), or the EcoRI-SalI site of pEGFP-N1 (Clontech).

A firefly luciferase reporter plasmid was constructed as follows. The fragments (−231 to −146) with wild-type and mutated 7 bp in R2 region were generated by PCR using the template DNA, pHISi-R2, and the primer pairs 5′-AAAACGCGTAATCATGCTGGCCGGCGT-3′/5′-AAACTCGAGCCCCACGGCGCCTTGCGTCCCAGA-3′ and 5′-AAAACGCGTAATCATGCTGGCAAGCGTGGCCCCGCCTCCGCAAGCGCGGCCCCGCCTCCGCAAGCGCAGCGTCT-3′/5′-AAACTCGAGCCCCACGGCGCCTTGCGTCCCAGA-3′ (mutations are underscored), respectively.

Each amplified fragment (wt-7bp and m3-7bp) was digested with MluI and XhoI and inserted into pGV-E2 reporter vector (Toyo Inc.), resulting in two reporter constructs, pGV-E2-wt-7bp/Luc and pGV-E2-m3-7bp/Luc.

Electrophoretic Mobility Shift Assays (EMSA)—A series of the GST-fused HDBP1 and HDBP2 was expressed in *Escherichia coli* strain BL21(DE3)-pLysS in the presence of 0.1 mM isopropyl-1-thio-β-D-galactopyranoside and 100 μM zinc chloride, and purified using GSTrap (Amersham Biosciences) according to the protocol from the manufacturer. Probe DNAs were prepared by digesting the pHISi-1 plasmid containing R1, R2, R3, or R4 fragments with the EcoRI-MluI site and the pGV-E2 plasmid containing wt-7bp or m3-7bp fragment with the MluI-XhoI site and then labeled with [α-^{32}P]dATP and [α-^{32}P]dCTP using DNA polymerase Klenow fragment (Takara Bio Inc.), respectively.

Binding reaction was performed in binding buffer (20 mM Tris-HCl (pH 7.6), 50 mM KCl, 10% glycerol, 1 mM DTT, 2 μg poly(dI-dC)·poly(dI-dC) (Amersham Biosciences)). GST fusion proteins were incubated in binding buffer for 5 min at room temperature with or without competitor DNAs. The ^{32}P-labeled probe (0.1 ng) was then added and incubated for another 20 min at room temperature. DNA-protein complexes were resolved on 4% polyacrylamide gels in 0.5× TBE (45 mM Tris borate, 1 mM EDTA) at 120 V for 2 h. Gels were dried under vacuum and exposed to Kodak x-ray film.

DNase I Footprinting—The 253-bp DNA fragment of the *HD* promoter region was amplified by PCR using primer pair 5′-AAAACGCGTGTTGAGCCCCGCGCCTTCG-3′ and 5′-AAAACTCGAGAGCGGCCGTCCATCTTGGA-3′, and cloned using a TA cloning system (Invitrogen), followed by digestion with MluI and XhoI. The MluI-XhoI fragment was isolated, end-labeled with ^{32}P, and used for DNase I footprinting. Binding reaction was performed in a total volume of 20 μl of binding buffer (20 mM Tris-HCl (pH 7.6), 50 mM KCl, 10% glycerol, 1 mM DTT, 2 μg poly(dI-dC)·poly(dI-dC) (Amersham Biosciences)). The ^{32}P-end-labeled DNA fragment (1 ng) was mixed with GST-HDBPs-C (10, 50, 200, and 400 ng) and incubated for 20 min at room temperature. Two μl of 10× DNase I solution (15 μg/ml DNase I, 50 mM $MgCl_2$) was added, incubated for additional 1 min at 25 °C, and followed by the addition of DNase I stop solution (1.6 M ammonium acetate, 95 mM EDTA, 0.8% SDS, 0.3 mg/ml calf thymus DNA). The DNA mixture was treated with phenol-chloroform and precipitated with ethanol. Precipitated DNA was dissolved in loading dye (80% formamide, 10 mM EDTA (pH 8.0), 0.025% bromphenol blue, 0.025% xylene cyanol). The samples were electrophoresed on an 8 M urea, 8% acrylamide gel. Sequence ladders (G+A and T+C) were generated by standard chemical sequencing techniques of Maxam and Gilbert.

Measurement of Reporter Gene Activity by Luciferase Assay—HeLa and IMR32 cells were cultured in Dulbecco's modified Eagle's medium (Invitrogen) and minimum essential medium (Invitrogen) with 10% fetal bovine serum (FBS) in 5% CO_2 humidified atmosphere at 37 °C, respectively. Cells were plated by 36 h before transfection at a density of 1×10^5 cells/well (HeLa) and 1×10^6 cells/well (IMR32) in 6-well culture plates. HeLa and IMR32 cells were transfected with 100 and 500 ng of pGV-E2-wt-7bp/Luc or -m3-7bp/Luc and 5 and 25 ng of pRL-TK (Nippon Gene) using FuGENE6 transfection reagent (Roche Applied Science), respectively. After incubation for 24 h, cells were washed with phosphate-buffered saline and lysed with 1× lysis buffer (Promega). Luciferase assays were carried out according to the protocol from the manufacturer using the dual luciferase reporter assay system (Promega) and TR717 Microplate Luminometer (PerkinElmer Applied Biosystems). The firefly luciferase activity was normalized to the control sea pansy luciferase activity to control for variations in transfection efficiency (24).

Subcellular Localization Analysis of GFP Fusion Proteins—HeLa cells were plated by 18 h before transfection at a density of 0.8×10^4 cells/well on an 8-well chamber slide (Becton Dickinson) and were

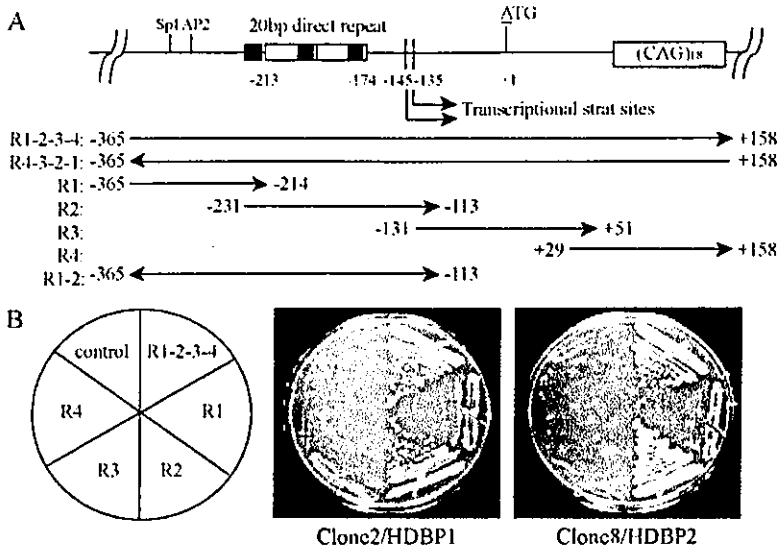

FIG. 1. **Identification of the candidate transcription factors for the *HD* gene using a yeast one-hybrid system.** *A*, schematic representation of the 5′-flanking region and exon 1 of the *HD* gene. Positions of the bait DNA fragments used in the generation of the yeast reporter strains are shown. R1-2-3-4 spans the region between nucleotides −365 and +158 (GenBank™ accession nos. L34020 and Y07981). Potential Sp1 and AP2 binding sites within the R1 region between nucleotides −365 and −214 have been reported. Two copies of 20-bp direct repeat (*gray boxes*) and two transcriptional start sites, both of which are present within the R2 region between nucleotides −231 and −113, are also shown. R3 and R4 contain a portion of exon 1 of the *HD* gene, spanning the regions between nucleotides −131 and +51 and between nucleotides +29 and +158, respectively. The number of the CAG repeat in the R4 fragment is 18 repeats. Adenine of the translation start site (ATG) is *numbered* as *+1*. *Three filled boxes* indicate 7-bp protected core sequences (GCCGGCG: HDBP1 and HDBP2 binding sites) found by DNase I footprinting (see Fig. 6). *B*, four yeast reporter strains carrying a bait DNA fragment of R1-2-3-4, R1, R2, R3, or R4 were used for the yeast one-hybrid assay. Each reporter strain was re-transformed with plasmid DNA of pACT2 clone 2/HDBP1 or pACT2 clone 8/HDBP2, and was cultured on SD/−His/−Leu medium containing 45 mM 3-AT. A yeast reporter strain that was transformed with pHISi-1 empty-vector alone was used as a control.

transfected with 1 μg of the pHDBP-GFP expression plasmids using an Effectene™ transfection reagent (Qiagen). IMR32 cells were plated by 36 h before transfection at a density of 2.5×10^5 cells/well on 2-well chamber slide (Nunc) and were transfected with 1 μg of the pHDBPs-GFP expression plasmids using FuGENE 6 transfection reagent (Roche Applied Science). After 24 h, HeLa and IMR32 cells were fixed with 4% paraformaldehyde, and were examined for subcellular localization of GFP fusion proteins under a fluorescence microscopic observation (DM-REB; Leica) and confocal microscopic observation (TCS_NT confocal microscope systems; Leica), respectively. To examine effects of leptomycin B, transfected cells were treated with 10 ng/ml leptomycin B for 1 h after 24 h of transfection.

Mutagenesis of the HDRF1 and HDRF2 Clones—Two amino acid substitution mutations were introduced into pHDBP1-MycHis and pHDBP2-MycHis by GeneEditor™ *in vitro* site-directed mutagenesis system (Promega) using the following mutagenic oligonucleotides: hdrf1 (L257A/L260A), 5′-GATGTTGGTGTGGACACGCTGACCGACG-GGGCGTCCAGCGCGACTCCAGTGTCCCCCACGGCCTCCATGCCG-3′; hdrf1 (F273A/L276A), 5′-GTGTCCCCCACGGCCTCCATGCCGCCT-GCCGCCCCCCGCGCCGGAGCTGCCAGAGCTGCTGGAGCCCCCAGC-C-3′; hdrf2 (L109A/L113A), 5′-TGGATGGAGGGTCAGGTGACCGTCT-GGCTGGCGGAGCAGAAGGCGCAGGTCTGCTGCAGGGTGGAGGA-GGTGTGG-3′; hdrf2 (M169A/M172A), 5′-GAAGTCGGACGCAGTGGA-AATGGATGAGATGGCGGCGGCCGCGGTGCTGACGTCCCTGTCCT-GCAGCCCTGTTG-3′ (mutations are underscored). The resulting mutants, pHDBP1(L257A/L260A)-MycHis, pHDBP1(F273A/L276A)-MycHis, pHDBP2(L109A/L113A)-MycHis, and pHDBP2(M169A/M172A)-MycHis, were confirmed by DNA sequencing analysis. To generate GFP fusion expression constructs with mutations, the fragments were amplified from pHDBP1(L257A/L260A)-MycHis and pHDBP1(F273A/L276A)-MycHis using the primer pair hdrf1gF/hdrf1gR, and from pHDBP2(L109A/L113A)-MycHis and pHDBP2(M169A/M172A)-MycHis using the primer pair hdrf2F/hdrf2R. Each fragment was digested with EcoRI and SalI and inserted into the EcoRI-SalI site of pEGFP-N1 vector (Clontech), resulting in pHDBP1(L257A/L260A)-GFP, pHDBP1(F273A/L276A)-GFP, pHDBP2(L109A/L113A)-GFP, and pHDBP2(M169A/M172A)-GFP.

RESULTS

Identification of Proteins That Bind to the Promoter Region of the HD Gene—To explore the promoter-binding proteins of the

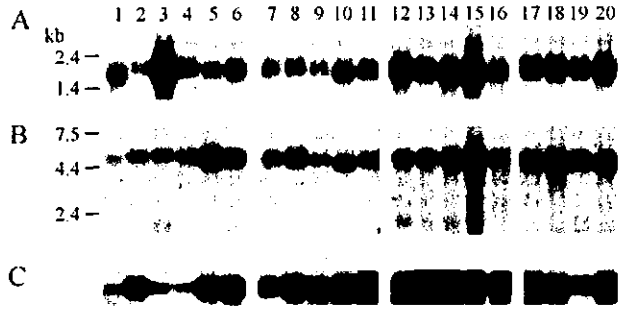

FIG. 2. **Northern blot analysis of mRNAs encoding HDBP1 and HDBP2.** Northern blots of mRNA from various adult human tissues were hybridized with the 1.3-kb cDNA fragment of HDBP1 (*A*), the 1.7-kb cDNA fragment of HDBP2 (*B*), and human β-actin cDNA (*C*) as probes. Molecular size markers are indicated in kb on the *left*. *Lane 1*, heart; *lane 2*, brain; *lane 3*, liver; *lane 4*, pancreas; *lane 5*, placenta; *lane 6*, lung; *lane 7*, stomach; *lane 8*, jejunum; *lane 9*, ileum; *lane 10*, colon; *lane 11*, rectum; *lane 12*, muscle; *lane 13*, uterus; *lane 14*, bladder; *lane 15*, kidney; *lane 16*, spleen; *lane 17*, cervix; *lane 18*, ovary; *lane 19*, testis; and *lane 20*, prostate.

HD gene, we performed a yeast one-hybrid screening with a human testis Matchmaker cDNA (GAL4 activation domain) library using a yeast reporter strain containing the bait R1-2-3-4 DNA fragment (Fig. 1*A*). Thirty-three positive clones (pACT2 clones) have been isolated so far. Five of these clones represented the same cDNA (pACT2 clone 2, ~1.3-kb cDNA size, GenBank™ accession no. AB044786) (Fig. 1*B*), and the other two clones represented independent cDNAs, pACT2 clone 8 (~1.7-kb cDNA size, GenBank™ accession no. AB044750) (Fig. 1*B*) and pACT2 clone 11, respectively.[2] The rest of 26 clones are false positives, which neither carry in-frame coding

[2] K. Tanaka, J. Shouguchi-Miyata, N. Miyamoto, and J.-E Ikeda, unpublished data.